Arabian Journal of Chemistry (2016) xxx, xxx–xxx

King Saud University

Arabian Journal of Chemistry

www.ksu.edu.sa
www.sciencedirect.com

ORIGINAL ARTICLE

Synthesis, structure elucidation, determination of antiproliferative activities, lipophilicity indices and pharmacokinetic properties of novel fused azaisocytosine-like congeners

Małgorzata Sztanke [a,*], **Jolanta Rzymowska** [b], **Małgorzata Janicka** [c], **Krzysztof Sztanke** [d]

[a] *Department of Medical Chemistry, Medical University, 4A Chodźki Street, 20-093 Lublin, Poland*
[b] *Department of Biology and Genetics, Medical University, 4A Chodźki Street, 20-093 Lublin, Poland*
[c] *Department of Physical Chemistry, Faculty of Chemistry, Maria Curie-Skłodowska University, Maria Curie-Skłodowska Sq. 3, 20-031 Lublin, Poland*
[d] *Laboratory of Bioorganic Synthesis and Analysis, Department of Medical Chemistry, Medical University, 4A Chodźki Street, 20-093 Lublin, Poland*

Received 6 February 2016; accepted 7 April 2016

KEYWORDS

Fused azaisocytosine-containing congeners;
Structure assignment;
Antiproliferative activities;
Retention factors;
Principal component analysis;
In silico bioactivity descriptors

Abstract The aims of the present study were the synthesis, an original spectroscopic characterization, an evaluation of antiproliferative activities and lipophilicity indices along with pharmacokinetic properties of a novel class of fused azaisocytosine-containing congeners. An optimized, well-established and scalable general method for the synthesis of the target molecules (**10–18**) *via* the [4 + 2] annulation strategy was worked out successfully, which enables reacting the molar equivalents of 1-aryl-2-hydrazinylideneimidazolidine hydroiodides (**1–9**) and ethyl 4-nitrophenylglyoxylate upon gently heating in *n*-butanol containing triethylamine and further refluxing in a solvent mixture *n*-butanol/DMF. The synthesis was hypothesized to proceed *via* ketimine intermediates that undergo intramolecular cyclization. All the synthesized compounds (**10–18**) revealed antiproliferative effects in four tumour cell lines of the epithelial origin, exerting superior cytotoxic activities in A549, HeLa and T47D cells to that of a reference drug – pemetrexed. Especially the **12**, **13**, **14**, **15** and **18** seem to be the most promising lead structures for designing more selective cytotoxic agents as they have a lower toxicity for normal epithelial cells after 24-h incubation period. In addition, a number of the innovative antimetabolite-type molecules have been

* Corresponding author. Tel.: +48 81 4486195.
E-mail address: malgorzata.sztanke@umlub.pl (M. Sztanke).

Peer review under responsibility of King Saud University.

ELSEVIER Production and hosting by Elsevier

http://dx.doi.org/10.1016/j.arabjc.2016.04.002

preselected that possess the optimum lipophilicity range significantly correlated with some *in silico* bioactivity descriptors relevant to the satisfactory pharmacokinetic profile *in vivo*. Thus, these original molecules might be useful as drug discovery leads to an early phase of drug design.

1. Introduction

Cancer is still considered to be the second "killer" (after heart disease) in the developed countries (Patrick, 2009). On the other hand, in clinical treatment there is still a lack of cytotoxic agents that are selective for neoplastic versus normal cells in spite of current progress in chemotherapy of certain human tumours. An application of new cytotoxic (antiproliferative) agents in patients suffering from cancer is also limited because of their harmful effects on the normal dividing cells as well as by overlapping severe side effects of combined anticancer drugs that are recently used in adjuvant chemotherapy (Denny, 2001). Therefore, the rational design and development strategy allowing for the prioritization of novel synthetic anticancer agents that show a selective cytotoxicity for cancer over normal cells seems to be of great urgency in the continuous search for novel more effective as well as more safer cytotoxic agents.

A number of small molecular weight structures based upon the privileged 7,8-dihydroimidazo[2,1-*c*][1,2,4]triazin-4(6*H*)-one template with the common phenyl moiety at the *C*-3 and the modified aryl substitution patterns at the *N*-8 have previously been shown to possess remarkable antileukemic as well as antimetastatic activities (Fig. 1, the structures **I–VII**) (Sztanke et al., 2009). The promising substituents attached at the *N*-8 of this template such as: 4-$MeOC_6H_4$ in **I**, monochloro-substituted phenyl moieties (mostly 2-ClC_6H_4 in **II** and 4-ClC_6H_4 in **III**) and dichloro-substituted phenyls (3,4-$Cl_2C_6H_3$ in **IV** and 2,5-$Cl_2C_6H_3$ in **V**) have previously been identified as beneficial for the antileukemic potency. In turn, some structures (e.g., those with 4-$MeOC_6H_4$ (**I**), 3-MeC_6H_4 (**VI**) and monochlorophenyl substitutions such as 2-ClC_6H_4 (**II**), 3-ClC_6H_4 (**VII**) and 4-ClC_6H_4 (**III**)) have previously been described as capable of evoking significant antimetastatic activities in human cervical epithelial cancer cells. Finally, the modification at the *N*-8 portion of the privileged imidazotriazinone scaffold in this class of compounds, followed by extensive *in vitro* testing, has led to the drug discovery lead (**III**), in which the 4-chlorophenyl moiety was identified as the best substitution pattern for the enhanced selectivity. This compound is deprived of cytotoxic effects towards normal cells, evokes enhanced dose-dependent viability decreases in human myeloma cells and is of importance due to the anticipated antimetastatic potential in human cervical epithelial cancer cells, as previously described (Sztanke et al., 2009). The same lead structure (conformationally stable and currently being investigated as potential drug candidate) has previously been proposed as useful for the subsequent design of lower toxic anticancer agents from this class of isosteric isomers of fused azacytosine-like congeners.

In view of the above findings and continuing our studies (Sztanke et al., 2009, 2015; Janicka et al., 2013), we have designed antimetabolite-type fused azaisocytosine-like congeners. Our interest in these compounds results from their structural novelty, the possibility of introducing various electron-donating and electron-withdrawing substituents at the aromatic phenyl ring and the anticipated biological activity as well as bioavailability. Therefore, the aim of the present study was to develop an optimized and effective approach leading to the synthesis of unknown angular nitrogen bicyclic molecules containing azaisocytosine-template (**10–18**) in order to perform, for the first time, the investigations concerning their complete spectroscopic, antiproliferative, lipophilic and pharmacokinetic properties.

Previous studies have found that antitumour active antimetabolite, azacytidine, is readily deaminated *in vivo* to inactive 6-azauridine by cytidine deaminase, whereas azaisocytosine is resistant to this enzyme (Hwang et al., 1995; Pitha et al., 1966). Therefore, we have designed a novel class of the compounds (e.g., fused azaisocytosine-containing congeners) that as derivatives of the isosteric isomers of 6-azacytosine (that could probably be utilized as false building blocks required for the DNA synthesis) may be of chemical as well as medical relevance due to their anticipated resistance to cytidine deaminase. Thus, the particular importance in these original molecules results

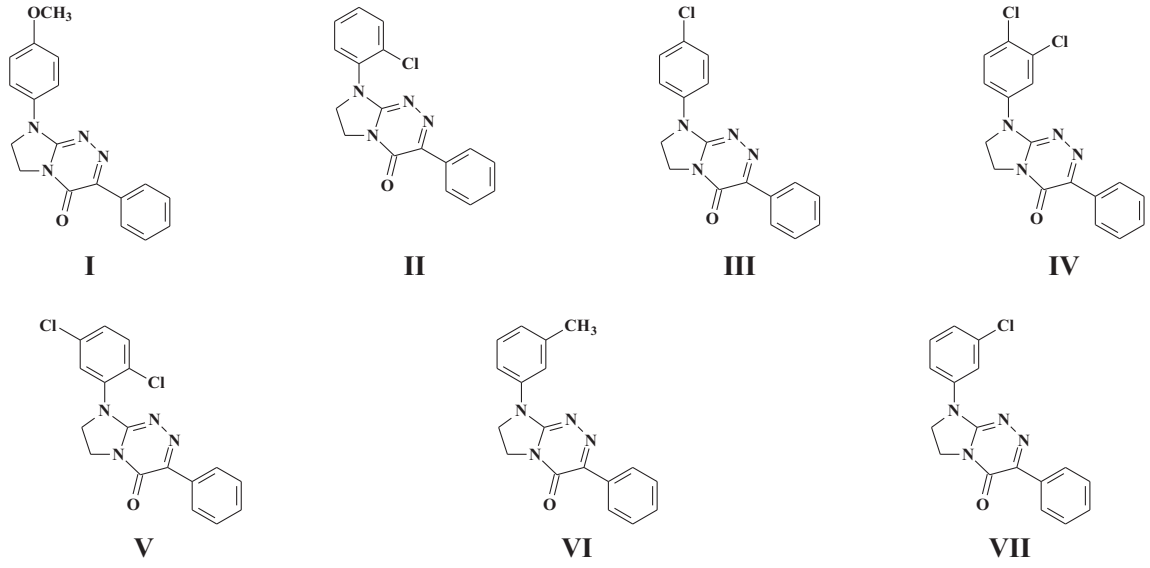

Figure 1 Previously reported (Sztanke et al., 2009) polynitrogenated bicyclic molecules comprising in their structures fused azaisocytosine template.

from their potential possibility of therapeutic use as innovative antimetabolites for combating cancer. All the designed molecules, featuring modified substitution sites at the *C*-3 (e.g., *para*-nitrophenyl) and the *N*-8 (e.g., phenyl and variously substituted phenyl moieties) positions, are based on the drug-like 7,8-dihydroimidazo[2,1-*c*][1,2,4] triazin-4(6*H*)-one template (Sztanke et al., 2009). This seems to be an extremely good scaffold for the design of novel adenosine receptor antagonists that may be of the anticipated benefit in the therapy of diseases associated with angiogenesis, such as cancer and diabetic retinopathy (Keisuke et al., 1993; Taliani et al., 2012) and in the treatment and prevention of inflammatory diseases, mainly hepatic cirrhosis (Szuster-Ciesielska et al., 2012; Kandefer-Szerszeń et al., 2014). The selection of a substitution pattern on the phenyl ring at the *N*-8 of the privileged scaffold in this novel class of compounds is stringently based on prior scientific literature evidence (Sztanke et al., 2009, 2015) and the synthetic approach is carried out to obtain innovative antimetabolite-type molecules, revealing not only antiproliferative effects against tumour cells but foremost a lower toxicity towards normal cells. The choice of the introduced *para*-nitrophenyl moiety at the *C*-3 is based on previous research findings, which showed that this moiety is capable of significantly enhancing antiproliferative activities of successful antimetabolite-type analogues (Brulíková et al., 2011). Moreover, it has been reported that some nitroaromatic-containing molecules as tumour-activated prodrugs may be selectively activated in cancerous tissue (Denny, 2001).

The aim of our cell-based anticancer investigations is to identify novel antiproliferative active lead structures revealing more selectivity for malignant (A549, HeLa, T47D and TOV112D) over normal (Vero) cells of the same epithelial origin.

The novel aspect of our chromatographic measurements is to assess the utility of three types of RPLC columns (IAM, cholesterol and ISRP) with different stationary materials in systematic studies of the lipophilicity of a novel class of molecules. The subsequent purpose of these studies is to check the possibility of processing the determined isocratic retention factors (logs *k*) in rational bioavailability predictions (log $BB_{permeation}$, log $BB_{distribution}$, log K_{HSA}, %F, $f_{u,\ plasma}$, Caco-2, $P_{e,\ jejunum}$) that were performed to identify novel lead structures with an optimum lipophilicity range that allows their satisfactory pharmacokinetics. Moreover, principal component analysis is employed with the goal of visualizing trends in data matrixes of chromatographic, partitioning and pharmacokinetic parameters characterizing the title compounds (**10–18**).

2. Experimental protocols

2.1. Instrumentations and materials

Ethyl 4-nitrophenylglyoxylate of 98% purity was supplied from Alfa-Aesar GmbH (Germany) and was sufficiently pure to be used directly without further purification. Triethylamine (Et_3N) (Sigma–Aldrich, Germany) was dried over anhydrous potassium hydroxide and distilled before use. Anhydrous solvents for the synthesis (e.g., *n*-butanol, *N,N*-dimethylformamide, methanol) were purchased from Roth (Germany) and Merck (Germany) companies. Additionally, the polar solvents, such as a distilled water and methanol, were used to remove successfully a soluble by-product derived from the synthetic approach, e.g., triethylammonium iodide which was the explicitly better soluble in these solvents than were the isolated solid final products (**10–18**). A Heidolph rotary evaporator (Germany), working under reduced pressure, was used to concentrate the volatile components of the reaction mixture to a suitable volume after the completion of the synthesis process. Melting point (m.p.) of each novel congener was determined on a Boetius apparatus (Germany) and the given value is uncorrected. The purity of each compound was checked by thin-layer chromatography. For this aim the routine preparative TLC analysis was carried out on commercial Merck 0.2 mm SiO_2 gel aluminium sheets (60 F-254) with a fluorescence indicator that allows to visualize of each final product spot under UV light at an excitation wavelength of 254 nm. The combustion microanalyses for each element analyzed (C, H, Cl, N) were consistent within ±0.4% of the theoretical values. ^{1}H NMR spectra (that were observed at 300 MHz for ^{1}H nuclei) and ^{13}C NMR spectra (that were observed at 75 MHz for ^{13}C nuclei) for all novel compounds of this class (**10–18**) dissolved in deuterated dimethyl sulfoxide (DMSO-d_6) were carried out on a Bruker Avance 300 MHz spectrometer. DEPT-135 experiments were done additionally to fully assign carbon multiplicities for all the molecules that were analyzed. All the chemical shifts are given as δ values that were downfield in relation to an internal standard, e.g., tetramethylsilane (TMS) (δ = 0.00 ppm). Chemical shifts are provided in parts per million (ppm), whereas the magnitudes of coupling constants are reported in frequency units, e.g., hertz (Hz). Signal multiplicities, used to describe signals, are indicated as follows: s, singlet; d, doublet; t, triplet and m, multiplet. The reported retention times (t_R) of solutes **10–18** were determined on IAM column in 20 °C (293 K), using as a mobile phase 50% acetonitrile in the buffer adjusted to pH 7.4.

2.1.1. 1-Aryl-2-hydrazinylideneimidazolidine building blocks (*1–9*)

The patented earlier biologically active and stable at room temperature hydroiodide salts of 1-aryl-2-hydrazinylideneimi dazolidines (**1–9**) (Sztanke, 2012) were employed as strongly nucleophilic species. They were sufficiently pure to be used directly in synthesis of the presented herein fused azaisocytosine-like congeners.

2.1.2. A general procedure for the synthesis of a novel class of 3-(4-nitrophenyl)-8-aryl-7,8-dihydroimidazo[2,1-c] [1,2,4]triazin-4(6H)-ones (*10–18*)

1-Aryl-2-hydrazinylideneimidazolidine hydroiodide (0.02 mol) was suspended in 10 mL of *n*-butanol. Then, a slight molar excess of dry triethylamine (2.9 mL) and the molar equivalent of *para*-nitrophenylglyoxylate (0.02 mol) were added. The synthetic process was conducted in the first instance by gently heating of the starting reagents with stirring until the intermediate which appeared had fully crystallized. Then a relevant amount of DMF was added until a complete intermediate solid dissolution was accomplished during heating and stirring. Thermal cyclocondensation proceeded on refluxing in the resulting solvent mixture *n*-butanol-DMF with stirring, and its progress was monitored by preparative TLC that showed the process to be complete in 1–5 h. The boiling solution of reaction mixture was filtered off to remove sparse insoluble impurities and subsequently was concentrated to ca. half its volume by evaporation of the volatiles under reduced pressure. After cooling the concentrated mixture was subsequently kept refrigerated, a complete precipitation of the final product occurring after 3 h. Then a portion of the formed crude product was filtered off, washed sequentially with three treatments of water (5 mL) and with one or two treatments of cold methanol (5 mL), and finally purified by recrystallization from the solvent mixture DMF-methanol in the proportion as indicated

Please cite this article in press as: Sztanke, M. et al., Synthesis, structure elucidation, determination of antiproliferative activities, lipophilicity indices and pharmacokinetic properties of novel fused azaisocytosine-like congeners. Arabian Journal of Chemistry (2016), http://dx.doi.org/10.1016/j.arabjc.2016.04.002

below. The precipitate obtained after cooling was filtered off again, and finally dried using a dry heat sterilizer (MOV-212S-PE, Panasonic, Japan). The following novel compounds (that are given underneath) were obtained in a pure solid state by this general procedure.

*2.1.2.1. 3-(4-Nitrophenyl)-8-phenyl-7,8-dihydroimidazo[2,1-c][1,2,4]triazin-4(6H)-one (**10**)*. Obtained in 69% yield, when recrystallized from the solvent mixture DMF-MeOH (5:1) had m.p. 291–293 °C. Anal. Calcd for $C_{17}H_{13}N_5O_3$: C, 60.89; H, 3.91; N, 20.89. Found: C, 61.10; H, 3.90; N, 20.81. ^{1}H NMR (300 MHz, DMSO-d_6): δ 4.26 (s, 4H, $2CH_2$), 7.18–8.46 (m, 9H, aromatic protons: 5H, phenyl-H and 4H, 4-nitrophenyl-H); ^{13}C NMR (75 MHz, DMSO-d_6): δ 40.5 (C-6, CH_2), 45.5 (C-7, CH_2), 119.1 (2CH), 123.3 (2CH), 124.0 (CH), 128.5 (2CH), 128.9 (2CH), 138.4 (C-1″), 139.9 (C-1′), 145.5 (C-4″), 147.4 (C-3), 151.7 (C-8a), 152.1 (C-4); HPLC $_{IAM\ 293K}$ (50% acetonitrile in buffer pH 7.4): t_R = 1.54 min.

*2.1.2.2. 3-(4-Nitrophenyl)-8-(2-methylphenyl)-7,8-dihydroimidazo[2,1-c][1,2,4]triazin-4(6H)-one (**11**)*. Obtained in 53% yield, when recrystallized from the solvent mixture DMF-MeOH (3:1) had m.p. 210–211 °C. Anal. Calcd for $C_{18}H_{15}N_5O_3$: C, 61.89; H, 4.33; N, 20.05. Found: C, 61.67; H, 4.34; N, 19.98. ^{1}H NMR (300 MHz, DMSO-d_6): δ 2.31 (s, 3H, CH_3), 4.07–4.36 (m, 4H, $2CH_2$), 7.31–8.39 (m, 8H, aromatic protons: 4H, 2-methylphenyl-H and 4H, 4-nitrophenyl-H); ^{13}C NMR (75 MHz, DMSO-d_6): δ 17.5 (CH_3), 41.6 (C-6, CH_2), 48.0 (C-7, CH_2), 123.3 (2CH), 126.9 (CH), 126.9 (CH), 127.1 (CH), 128.3 (2CH), 131.0 (CH), 136.0 (C-2'), 136.1 (C-1″), 140.2 (C-1′), 144.5 (C-4″), 147.1 (C-3), 151.9 (C-8a), 153.2 (C-4); HPLC $_{IAM\ 293K}$ (50% acetonitrile in buffer pH 7.4): t_R = 1.84 min.

*2.1.2.3. 3-(4-Nitrophenyl)-8-(4-methylphenyl)-7,8-dihydroimidazo[2,1-c][1,2,4]triazin-4(6H)-one (**12**)*. Obtained in 72% yield, when recrystallized from the solvent mixture DMF-MeOH (9:1) had m.p. 278–280 °C. Anal. Calcd for $C_{18}H_{15}N_5O_3$: C, 61.89; H, 4.33; N, 20.05. Found: C, 62.11; H, 4.32; N, 20.11. ^{1}H NMR (300 MHz, DMSO-d_6): δ 2.33 (s, 3H, CH_3), 4.24 (s, 4H, $2CH_2$), 7.28 (d, J = 8.4 Hz, 2H, aromatic protons: 4-methylphenyl-H-2′ and H-6′), 7.77 (d, J = 8.5 Hz, 2H, aromatic protons: 4-methylphenyl-H-3′ and H-5′), 8.30–8.45 (m, 4H, aromatic protons: 4-nitrophenyl-H); ^{13}C NMR (75 MHz, DMSO-d_6): δ 20.4 (CH_3), 40.5 (C-6, CH_2), 45.6 (C-7, CH_2), 119.2. (2CH), 123.3 (2CH), 128.5 (2CH), 129.4 (2CH), 133.2 (C-4′), 136.0 (C-1″), 140.0 (C-1′), 145.2 (C-4″), 147.3 (C-3), 151.7 (C-8a), 152.1 (C-4); HPLC $_{IAM\ 293K}$ (50% acetonitrile in buffer pH 7.4): t_R = 1.34 min.

*2.1.2.4. 3-(4-Nitrophenyl)-8-(2,3-dimethylphenyl)-7,8-dihydroimidazo[2,1-c][1,2,4]triazin-4(6H)-one (**13**)*. Obtained in 55% yield, when recrystallized from the solvent mixture DMF-MeOH (2:1) had m.p. 274–276 °C. Anal. Calcd for $C_{19}H_{17}N_5O_3$: C, 62.80; H, 4.72; N, 19.27. Found: C, 62.58; H, 4.73; N, 19.20. ^{1}H NMR (300 MHz, DMSO-d_6): δ 2.19 (s, 3H, CH_3), 2.32 (s, 3H, CH_3), 4.06 (t, J = 8.9 Hz, 2H, CH_2), 4.31 (t, J = 8.9 Hz, 2H, CH_2), 7.19–7.32 (m, 3H, aromatic protons: 2,3-dimethylphenyl-H), 8.29 (d, J = 9.1 Hz, 2H, aromatic protons: 4-nitrophenyl-H), 8.38 (d, J = 9.1 Hz, 2H, aromatic protons: 4-nitrophenyl-H); ^{13}C NMR (75 MHz, DMSO-d_6): δ 14.1 (CH_3), 19.9 (CH_3), 41.5 (C-6, CH_2), 48.3 (C-7, CH_2), 123.3 (2CH), 124.7 (CH), 126.3 (CH), 128.3 (2CH), 129.6 (CH), 134.8 (C-2′), 136.1 (C-1″), 138.1 (C-3′), 140.3 (C-1′), 144.4 (C-4″), 147.1 (C-3), 151.9 (C-8a), 153.4 (C-4); HPLC $_{IAM\ 293K}$ (50% acetonitrile in buffer pH 7.4): t_R = 1.33 min.

*2.1.2.5. 3-(4-Nitrophenyl)-8-(2-methoxyphenyl)-7,8-dihydroimidazo[2,1-c][1,2,4]triazin-4(6H)-one (**14**)*. Obtained in 52% yield, when recrystallized from the solvent mixture DMF-MeOH (7:1) had m.p. 286–287 °C. Anal. Calcd for $C_{18}H_{15}N_5O_4$: C, 59.18; H, 4.14; N, 19.17. Found: C, 58.98; H, 4.15; N, 19.26. ^{1}H NMR (300 MHz, DMSO-d_6): δ 3.85 (s, 3H, OCH_3), 4.08 (t, J = 9.1 Hz, 2H, CH_2), 4.31 (t, J = 9.1 Hz, 2H, CH_2), 7.04–7.54 (m, 4H, aromatic protons: 2-methoxyphenyl-H), 8.30 (d, J = 9.1 Hz, 2H, aromatic protons: 4-nitrophenyl-H), 8.38 (d, J = 9.1 Hz, 2H, aromatic protons: 4-nitrophenyl-H); ^{13}C NMR (75 MHz, DMSO-d_6): δ 41.5 (C-6, CH_2), 47.3 (C-7, CH_2), 55.8 (CH_3O), 112.7 (CH), 120.6 (CH), 123.3 (2CH), 125.5 (C-1″), 128.3 (2CH), 128.5 (CH), 129.4 (CH), 140.2 (C-1′), 144.7 (C-4″), 147.2 (C-3), 151.8 (C-8a), 153.6 (C-4), 154.8 (C-2′); HPLC $_{IAM\ 293K}$ (50% acetonitrile in buffer pH 7.4): t_R = 1.58 min.

*2.1.2.6. 3-(4-Nitrophenyl)-8-(2-chlorophenyl)-7,8-dihydroimidazo[2,1-c][1,2,4]triazin-4(6H)-one (**15**)*. Obtained in 61% yield, when recrystallized from the solvent mixture DMF-MeOH (6:1) had m.p. 272–274 °C. Anal. Calcd for $C_{17}H_{12}ClN_5O_3$: C, 55.22; H, 3.27; Cl, 9.59; N, 18.94. Found: C, 55.01; H, 3.26; Cl, 9.56; N, 19.01. ^{1}H NMR (300 MHz, DMSO-d_6): δ 4.15 (t, J = 8.9 Hz, 2H, CH_2), 4.36 (t, J = 8.9 Hz, 2H, CH_2), 7.46–8.39 (m, 8H, aromatic protons: 4H, 2-chlorophenyl-H and 4H, 4-nitrophenyl-H); ^{13}C NMR (75 MHz, DMSO-d_6): δ 41.7 (C-6, CH_2), 47.7 (C-7, CH_2), 123.3 (2CH), 128.4 (2CH), 128.5 (CH), 129.9 (CH), 130.1 (CH), 130.3 (CH), 131.5 (C-2′), 134.8 (C-1″), 140.0 (C-1′), 145.3 (C-4″), 147.3 (C-3), 151.7 (C-8a), 153.5 (C-4); HPLC $_{IAM\ 293K}$ (50% acetonitrile in buffer pH 7.4): t_R = 1.39 min.

*2.1.2.7. 3-(4-Nitrophenyl)-8-(3-chlorophenyl)-7,8-dihydroimidazo[2,1-c][1,2,4]triazin-4(6H)-one (**16**)*. Obtained in 62% yield, when recrystallized from the solvent mixture DMF-MeOH (4:1) had m.p. 260–261 °C. Anal. Calcd for $C_{17}H_{12}ClN_5O_3$: C, 55.22; H, 3.27; Cl, 9.59; N, 18.94. Found: C, 43.14; H, 3.26; Cl, 9.57; N, 18.87. ^{1}H NMR (300 MHz, DMSO-d_6): δ 4.26 (s, 4H, $2CH_2$), 7.24–8.46 (m, 8H, aromatic protons: 4H, 3-chlorophenyl-H and 4H, 4-nitrophenyl-H); ^{13}C NMR (75 MHz, DMSO-d_6): δ 40.6 (C-6, CH_2), 45.4 (C-7, CH_2), 117.1 (CH), 118.6 (CH), 123.3 (2CH), 123.5 (CH), 128.7 (2CH), 130.6 (CH), 133.4 (C-1″), 139.6 (C-3′), 139.8 (C-1′), 146.0 (C-4″), 147.5 (C-3), 151.6 (C-8a), 152.0 (C-4); HPLC $_{IAM\ 293K}$ (50% acetonitrile in buffer pH 7.4): t_R = 1.40 min.

*2.1.2.8. 3-(4-Nitrophenyl)-8-(4-chlorophenyl)-7,8-dihydroimidazo[2,1-c][1,2,4]triazin-4(6H)-one (**17**)*. Obtained in 64% yield, when recrystallized from the solvent mixture DMF-MeOH (7:1) had m.p. 301–302 °C. Anal. Calcd for $C_{17}H_{12}ClN_5O_3$: C, 55.22; H, 3.27; Cl, 9.59; N, 18.94. Found: C, 55.39; H, 3.28; Cl, 9.59; N, 18.89. ^{1}H NMR (300 MHz, DMSO-d_6): δ 4.25 (s, 4H, $2CH_2$), 7.52–8.45 (m, 8H, aromatic

Please cite this article in press as: Sztanke, M. et al., Synthesis, structure elucidation, determination of antiproliferative activities, lipophilicity indices and pharmacokinetic properties of novel fused azaisocytosine-like congeners. Arabian Journal of Chemistry (2016), http://dx.doi.org/10.1016/j.arabjc.2016.04.002

protons: 4H, 4-chlorophenyl-H and 4H, 4-nitrophenyl-H); ^{13}C NMR (75 MHz, DMSO-d_6): δ 40.6 (C-6, CH_2), 45.4 (C-7, CH_2), 120.6 (2CH), 123.3 (2CH), 127.7 (C-4′), 128.6 (2CH), 128.8 (2CH), 137.4 (C-1″), 139.7 (C-1′), 145.8 (C-4″), 147.5 (C-3), 151.6 (C-8a), 152.0 (C-4); HPLC $_{IAM\ 293K}$ (50% acetonitrile in buffer pH 7.4): t_R = 1.83 min.

*2.1.2.9. 3-(4-Nitrophenyl)-8-(3,4-dichlorophenyl)-7,8-dihydroimidazo[2,1-c][1,2,4]triazin-4(6H)-one (**18**).* Obtained in 59% yield, when recrystallized from the solvent mixture DMF-MeOH (8:1) had m.p. 340–342 °C. Anal. Calcd for $C_{17}H_{11}Cl_2N_5O_3$: C, 50.51; H, 2.74; Cl, 17.54; N, 17.33. Found: C, 50.32; H, 2.73; Cl, 17.48; N, 17.27. ^{1}H NMR (300 MHz, DMSO-d_6): δ 4.25 (s, 4H, $2CH_2$), 7.71–8.45 (m, 7H, aromatic protons: 3H, 3,4-dichlorophenyl-H and 4H, 4-nitrophenyl-H); ^{13}C NMR (75 MHz, DMSO-d_6): δ 40.6 (C-6, CH_2), 45.4 (C-7, CH_2), 118.7 (CH), 120.2 (CH), 123.3 (2CH), 125.4 (C-4′), 128.7 (2CH), 130.7 (CH), 131.3 (C-3′), 138.5 (C-1″), 139.5 (C-1′), 146.2 (C-4″), 147.5 (C-3), 151.5 (C-8a), 151.9 (C-4); HPLC $_{IAM\ 293K}$ (50% acetonitrile in buffer pH 7.4): t_R = 2.34 min.

2.1.3. An assessment of DNA synthesis and cytotoxicity

The carried out determination is based on the measurement of the amount of the labelled synthetic nucleoside analogue, e.g., 5-bromo-2′-deoxyuridine (BrdUrd), incorporated into the cellular DNA in place of thymidine during the nascent synthesis phase in a panel of cells that were treated with the compounds of interest. Cells treated only with the culture media served as controls. A panel of four tumour cell lines (such as: A549 (ECACC 86012804) – human Caucasian lung carcinoma cells, HeLa (ECACC 93021013) – human Negroid cervix epitheloid carcinoma cells, T47D (ECACC 85102201) – human breast carcinoma cells and TOV112D (ATCC CRL-11731) – human ovarian malignant adenocarcinoma cells) and one normal cell line (e.g., Vero (ECACC 88020401) – African Green Monkey kidney cells) of the same epithelial origin were employed. The used cell lines were sourced and cultured as described in detail previously (Sztanke et al., 2015).

End-point determinations were performed on an enzyme-linked immunosorbent assay (ELISA) reader (BIO-TEC Instruments, USA) using a commercially available chemiluminescent BrdUrd labelling and detection kit III (Roche Diagnostics, Indianapolis, USA) (Muir et al., 1990; Ellwart and Dormer 1985; Magaud et al., 1988; Huong, 1991). Each freshly prepared stock solution of the screened compound in dimethyl sulfoxide (Sigma–Aldrich, Germany) of above 99.9% purity and filtered through an aseptic 0.22 μm-pore-size syringe filter (GE Water and Process Technologies, USA) was finally diluted into the cell culture media to obtain its 50 μg mL^{-1} concentration. The effect of each investigated solute at the tested concentration on the BrdUrd incorporation was assessed spectrophotometrically after 24-, 48- and 72-h periods of incubation at standard conditions (37 °C, 5% CO_2, 90% humidity) and compared to the untreated control cells. Table 1 specifies the percentage values of growth inhibition over a time in malignant and normal cells for all novel compounds of interest. These values were determined in the following manner: at first mean absorbance levels of at least three measurements taken from the repeated true independent BrdUrd-based evaluations were derived; then these mean values were converted into the per cent of growth inhibition. A well-known folate antimetabolite – pemetrexed (Lilly, Slovakia) at a concentration of 0.23 mM (100 μg mL^{-1}) was used as a positive control (Sztanke et al., 2015) for the DNA synthesis and cytotoxicity measurements.

2.1.4. Chromatographic measurements

2.1.4.1. Reagents and materials. Acetonitrile (MeCN) of HPLC grade was purchased from Merck (Darmstadt, Germany), whereas both citric acid and Na_2HPO_4 were certified as being of analytical purity and supplied from Avantor Performance Materials (Lublin, Poland). For HPLC measurements a double distilled water was used that was obtained using a Direct-Q 3 UV apparatus (Millipore, Warsaw, Poland). The buffer (used as a mobile phase component) was prepared from 0.01 mol L^{-1} solutions of Na_2HPO_4 and citric acid that were mixed together and finally filtered through a 0.45 μm-pore-size syringe filter (GE Water and Process Technologies, USA). It should be noted that the physiological pH value of resulting buffer solution (7.4) was achieved purposefully (as the corresponding to a normal blood pH range of humans, e.g., 7.35–7.45) before mixing with acetonitrile as an organic modifier.

2.1.4.2. HPLC experimental. HPLC measurements were performed employing a Shimadzu Vp (Shimadzu, Izabelin, Poland) liquid chromatographic system (which was equipped with columns packed with different reversed-phase materials as indicated below, a LC 10AT pump, a SPD 10A UV–VIS detector, a SCL 10A system controller, and a Rheodyne injector valve fitted with a 20 μL loop). All measurements were performed under the isocratic conditions at 20 °C (293 K) as well as 37 °C (310 K). The measurement temperatures were controlled by a CTO-10 AS chromatographic oven. In the investigations values of the peak asymmetry factor for each solute sample were in the acceptable range without none additional peaks on the registered chromatograms. Single peaks of the tested compounds were detected under middle ultraviolet (MUV) light at 254 nm. The dead time values were measured from the peaks of citric acid. The capacity factors were calculated from average values, that were taken from at least three independent experimental measurements. The following equation was employed to calculate the retention factor, k:

$$k = (t_R - t_0)/t_0$$

where t_R is the retention time of the original compound that was analyzed and t_0 denotes the dead time which was established by injection of a non-retained marker, e.g., citric acid.

For RPLC experiments three different stationary phases that were employed were as follows: the IAM column IAM. PC.DD2 100 × 4.6 mm i.d., 10 μm, manufacture number 43751 (Regis Chemicals Company, Morton Grove, Illinois, USA), the cholesterol column Cosmosil Cholester, 75 × 2 mm i.d., 2.5 μm, manufacture number R75182 (Genore, Warsaw, Poland) and the ISRP GFF II column, 150 × 4.6 mm i.d., 5 μm, manufacture number 53310 (Regis Chemicals Company, Morton Grove, Illinois, USA).

Buffer-acetonitrile mixtures were employed as mobile phases for RPLC measurements in which acetonitrile concentration in the effluent (expressed as a volume fraction) was equal to 0.4 φ and 0.5 φ, respectively. The prepared mobile phases were filtered through a 0.45 μm-pore-size syringe filter

Please cite this article in press as: Sztanke, M. et al., Synthesis, structure elucidation, determination of antiproliferative activities, lipophilicity indices and pharmacokinetic properties of novel fused azaisocytosine-like congeners. Arabian Journal of Chemistry (2016), http://dx.doi.org/10.1016/j.arabjc.2016.04.002

Table 1 Growth inhibition ratios of normal and tumour cells by an effective concentration of novel small molecular weight fused azaisocytosine-like congeners.

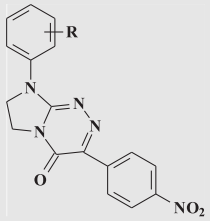

Compound	*R*	Incubation time	Growth inhibition (%)[a] in cell lines				
			Vero	A549	HeLa	T47D	TOV112D
10	H	24 h	40 ± 4.5	70 ± 7.2	80 ± 7.8	100 ± 12.2	80 ± 7.8
		48 h	95 ± 10.6	90 ± 8.9	90 ± 10.1	100 ± 9.9	100 ± 12.0
		72 h	100 ± 15.2	100 ± 12.4	100 ± 9.8	100 ± 10.6	100 ± 9.6
11	2-CH_3	24 h	50 ± 6.5	75 ± 8.0	80 ± 8.2	60 ± 5.8	80 ± 6.6
		48 h	75 ± 5.2	80 ± 7.9	90 ± 10.2	80 ± 7.9	90 ± 8.4
		72 h	95 ± 9.8	100 ± 11.4	100 ± 12.4	90 ± 8.9	100 ± 9.5
12	4-CH_3	24 h	10 ± 1.8	25 ± 2.4	85 ± 8.2	90 ± 10.2	80 ± 6.2
		48 h	80 ± 7.5	50 ± 5.6	90 ± 8.6	100 ± 10.6	90 ± 5.2
		72 h	100 ± 15.4	80 ± 7.9	100 ± 10.6	100 ± 12.1	95 ± 7.2
13	2,3-$(CH_3)_2$	24 h	15 ± 1.9	25 ± 3.0	75 ± 6.9	80 ± 7.8	50 ± 3.5
		48 h	50 ± 3.8	75 ± 8.1	85 ± 8.1	95 ± 8.6	90 ± 6.7
		72 h	90 ± 12.5	85 ± 8.0	90 ± 8.9	100 ± 10.8	100 ± 11.2
14	2-OCH_3	24 h	10 ± 1.5	30 ± 2.7	85 ± 7.9	80 ± 6.8	80 ± 6.8
		48 h	40 ± 5.6	75 ± 8.2	90 ± 10.5	90 ± 7.8	90 ± 8.8
		72 h	75 ± 5.2	80 ± 8.8	100 ± 9.6	100 ± 9.5	100 ± 9.7
15	2-Cl	24 h	15 ± 1.2	50 ± 4.8	65 ± 5.9	90 ± 6.8	80 ± 5.9
		48 h	50 ± 5.8	90 ± 8.9	80 ± 7.8	100 ± 9.2	100 ± 9.5
		72 h	80 ± 8.2	100 ± 11.8	100 ± 12.1	100 ± 8.6	100 ± 10.8
16	3-Cl	24 h	75 ± 6.8	80 ± 7.9	85 ± 7.9	95 ± 5.8	80 ± 6.9
		48 h	85 ± 7.9	100 ± 11.2	95 ± 9.5	100 ± 8.8	100 ± 8.8
		72 h	100 ± 9.2	100 ± 9.8	100 ± 10.9	100 ± 9.8	100 ± 9.4
17	4-Cl	24 h	50 ± 4.8	75 ± 6.8	85 ± 8.2	95 ± 8.2	90 ± 6.5
		48 h	100 ± 11.2	100 ± 9.8	90 ± 8.8	100 ± 11.7	100 ± 8.5
		72 h	100 ± 10.6	100 ± 10.6	100 ± 10.5	100 ± 10.4	100 ± 9.2
18	3,4-Cl_2	24 h	30 ± 3.2	80 ± 8.4	90 ± 7.8	95 ± 6.8	90 ± 7.5
		48 h	70 ± 7.4	100 ± 12.2	100 ± 8.9	100 ± 8.8	100 ± 9.2
		72 h	100 ± 12.5	100 ± 11.5	100 ± 10.5	100 ± 12.6	100 ± 7.5
A reference drug		24 h	5 ± 0.2	10 ± 0.9	5 ± 0.7	10 ± 0.8	nd
		48 h	10 ± 1.1	30 ± 2.4	10 ± 0.9	20 ± 1.2	nd
		72 h	20 ± 1.9	50 ± 2.8	20 ± 1.5	30 ± 2.2	nd

Normal epithelial cell line: Vero – (ECACC 88020401) – African Green Monkey kidney cells.
Cancer cell lines of the epithelial origin: A549 (ECACC 86012804) – human Caucasian lung carcinoma cells; HeLa (ECACC 93021013) – human Negroid cervix epitheloid carcinoma cells; T47D (ECACC 85102201) – human breast carcinoma cells; TOV112D (ATCC CRL-11731) – human ovarian primary malignant adenocarcinoma cells.
An effective concentration of 50 μg mL^{-1} corresponds to the following millimolar concentration values: 0.149 mM (**10**), 0.143 mM (**11, 12**), 0.138 mM (**13**), 0.137 mM (**14**), 0.135 mM (**15**, **16, 17**), 0.124 mM (**18**).
A reference drug – pemetrexed at a concentration of 100 μg mL^{-1} (0.23 mM) (Sztanke et al., 2015).
nd – not determined.
[a] Each value is the mean of at least three independent experiment values ± standard deviation.

(GE Water and Process Technologies, USA) before using them. Retention data were recorded at the flow rate of the following: 1.2 mL min^{-1} with the IAM column, 0.4 mL min^{-1} with the Cosmosil Cholester column and 0.6 mL min^{-1} with the ISRP column.

2.1.4.3. In silico calculations. The partition lipophilicities, expressed as log *P* values of the compounds of interest in the *n*-octanol–water system, as well as the molecular descriptors that are relevant to their pharmacokinetics (log $BB_{permeation}$, log $BB_{distribution}$, log K_{HSA}, %F, $f_{u,\ plasma}$, Caco-2, $P_{e,\ jejunum}$)

Please cite this article in press as: Sztanke, M. et al., Synthesis, structure elucidation, determination of antiproliferative activities, lipophilicity indices and pharmacokinetic properties of novel fused azaisocytosine-like congeners. Arabian Journal of Chemistry (2016), http://dx.doi.org/10.1016/j.arabjc.2016.04.002

were calculated using an ACD/Percepta software (Łódź, Poland). *In silico* calculations were carried out exploiting the Abraham's linear solvation energy relationships (Kaliszan, 2007; Vitha and Carr, 2006).

2.1.4.4. Statistical calculations. Multivariate data analyses, e.g., principal component and cluster variables analyses, and the regression analysis have been done using a chosen Minitab 16 statistical software (Minitab Inc., State College, Pennsylvania, USA).

3. Results and discussion

*3.1. Synthesis and spectroscopic characterization of a novel class of fused azaisocytosine-containing congeners (**10–18**)*

The patented biologically active 1-aryl-2-hydrazinylideneimida zolidines (**1–9**) (Sztanke, 2012) were exploited (as excellent nucleophilic centred building blocks) in synthesis of novel 3-(4-nitrophenyl)-8-aryl-7,8-dihydroimidazo[2,1-*c*][1,2,4]triazin-4(6*H*)-ones (**10–18**).

The target fused azaisocytosine-like congeners (**10–18**), comprising in their structures the incorporated 6-azaisocytosine template, were successfully prepared employing the general synthetic pathway, as shown in Scheme 1. An efficient and simple procedure has been developed that allows a patent pending synthetic approach of that novel class of compounds (Sztanke and Sztanke, 2014a,b). It is clear that in this case a new 1,2,4-triazinone template was annelated to the existing four atoms' fragment (N—C—N—N) of nucleophilic centred hydrazinylideneimidazolidines employing ethyl *para*-nitrophenylglyoxylate (as an excellent electrophilic donor of the two carbon atoms' fragment (C—C═O)) according to the [4 + 2] pattern (Rusinov et al., 2008). For this purpose, the molar equivalents of the available hydroiodide salts of hydrazinylideneimidazolidines bearing various substitution patterns on the phenyl ring (**1–9**) were successfully treated with ethyl *para*-nitrophenylglyoxylate in the suitable reaction media under basic conditions. Initially, the condensation process was conducted by gently heating the above starting materials in *n*-butanol medium containing a small molar excess of triethylamine leading to the formation of suitable ketimine intermediates (drawn in square bracket in Scheme 1). In this case the nucleophilic attack of the most reactive exocyclic amino-type nitrogen of hydrazono moiety to the reactive electrophilic carbonyl carbon at the position next to the ester group took place. The step of condensation would be expected to proceed with a concomitant removal of water molecule, and additionally led to an evolution of the hydrogen iodide from the reaction mixture which had reacted with Et_3N to give triethylammonium

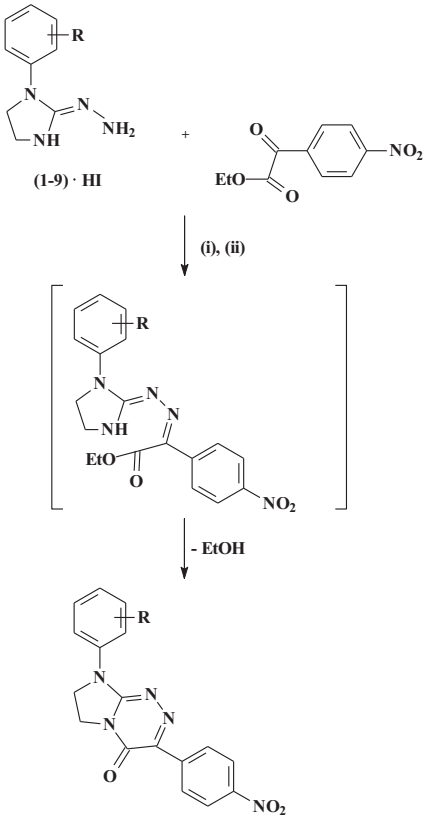

1,**10**: R = H; **2**,**11**: R = 2-CH_3; **3**,**12**: R = 4-CH_3; **4**,**13**: R = 2,3-$(CH_3)_2$; **5**,**14**: R = 2-CH_3O; **6**,**15**: R = 2-Cl; **7**,**16**: R = 3-Cl, **8**,**17**: R = 4-Cl; **9**,**18**: R = 3,4-Cl_2
Reagents and conditions: (i) *n*-BuOH, Et_3N, reflux, 2-10 min. (ii) *n*-BuOH/DMF, reflux, 1-5h

Scheme 1 A scheme for the synthesis of 3-(4-nitrophenyl)-8-aryl-7,8-dihydroimidazo[2,1-*c*][1,2,4]triazin-4(6*H*)-ones (**10–18**).

Please cite this article in press as: Sztanke, M. et al., Synthesis, structure elucidation, determination of antiproliferative activities, lipophilicity indices and pharmacokinetic properties of novel fused azaisocytosine-like congeners. Arabian Journal of Chemistry (2016), http://dx.doi.org/10.1016/j.arabjc.2016.04.002

iodide ($Et_3NH^+I^-$) as a by-product of alkylation. Subsequently, ketimine-type intermediates, containing the protonated endocyclic *N*3 nitrogen, are cyclized on heating in an inert refluxing *n*-butanol/DMF mixture to novel fused azaisocytosine-like congeners (**10–18**) with a concomitant loss of ethanol molecule. The results of combined ^{1}H NMR/^{13}C NMR investigations have fully defined the structures of final products that are based on the privileged 7,8-dihydroimidazo[2,1-*c*][1,2,4]triazin-4(6*H*)-one template. Moreover, the opposite mode of cyclization to 3-(4-nitrophenyl)-7-aryl-5*H*-6,7-dihydroimidazo[2,1-*c*][1,2,4]triazole derivatives (that has also been thoroughly investigated) proved to be impossible under the established reaction conditions since no traces of such type of compounds were detected in the clear spectroscopic data of the final products. It is now believed that thermal cyclization of intermediates to the desired products proceeds in the direction which yields the most stable cyclic products possessing the least energy.

The complete spectroscopic characterization of novel fused azaisocytosine-like congeners (**10–18**) is specified in Subsection 2.1.2. describing the experimental protocols. The title compounds (**10–18**) exhibited ^{13}C NMR chemical shifts of the *C*7 atoms at δ in the region 45.4–48.3 ppm, whereas the corresponding lower shifts of the *C*6 atoms were found to be at δ in the region 40.5–41.7 ppm. These findings proved that there are two endocyclic methylene groups (in the five-membered imidazolidine ring) that reveal an unequal chemical character. Obviously these secondary methylene carbon atoms (*C*6 and *C*7) were unambiguously identified as the signals that go down, when analysing the results of DEPT-135 experiment. ^{1}H NMR chemical shifts of the aromatic proton signals (derived from two rings attached to the bicyclic scaffold) were found to be at δ in the region 7.04–8.46 ppm, as indicated in the case of all the compounds (**10–18**). However, the compound **13** revealed the proton signals derived from the *para*-nitrophenyl ring (as two doublets in the aromatic region at δ 8.29 ppm and δ 8.38 ppm with coupling constants of J = 9.1 Hz and 9.1 Hz, respectively, integrating with two protons each) that were shifted the most downfield from those proton signals of the second 2,3-dimethylsubstituted phenyl ring (7.19–7.32 ppm).

In the present study we have optimized the general synthetic process by an adequate choice of reagents, solvents and suitable conditions that were required to synthesize the desired final products. It has been proved that the synthesis of novel fused-azaisocytosine-containing congeners (**10–18**), although conducted under mild conditions, proceeded with relatively good overall yields. Higher yields were obtained when the cyclization of the hypothetical intermediate ketimine-type Schiff bases was carried out for the suitable reaction period in refluxing *n*-butanol/DMF solvent mixture containing a small molar excess of Et_3N. The general synthetic procedure was developed in the present study on a multi-gram scale that could be applicable to a number of identifiable derivatives of this novel class.

Preparative procedures of the title compounds as well as reactions of 1-aryl-2-hydrazonoimidazolidine derivatives with ethyl *para*-nitrophenylglyoxylate have not been reported in the scientific literature yet, including Chemical Abstracts Service (CAS). Thus, this not studied in the past approach for the synthesis of an unknown class of fused azaisocytosine-like congeners (with the common 4-nitrophenyl moiety at the *C*-3 and different substitution patterns at the *N*-8) is the first time presented. As the synthesized compounds contain a nitro substitution on the aromatic phenyl ring they could be utilized in further synthesis of arylamines as well as aryldiazonic salts and their related derivatives.

The initial formation of the suitable ketimine-type Schiff bases, e.g., ethyl (2*Z*)-(4-nitrophenyl)[(2*E*)-(1-arylimidazolidin-2-ylidene)hydrazinylidene]acetates (**II**), as intermediates in the synthesis of final products (**10–18**), probably proceeds through an intermediate stage according to the mechanism that may be represented by Scheme 2. A nucleophilic attack of an amine-type nitrogen of the suitable hydrazinylideneimidazolidine to an electrophilic α-carbonyl carbon of ethyl *para*-nitrophenylglyoxylate results in the formation of hemiaminal (**I**), e.g., ethyl hydroxy(4-nitrophenyl)[(2*E*)-2-(1-arylimidazolidin-2-ylidene)hydrazinyl]acetate. Its further conversion into the suitable ketimine (**II**) followed with concomitant dehydration is accomplished by deprotonation of the nitrogen in hemiaminal molecule and pushing the oxygen off of the carbon by the electrons of the same nitrogen atom. The first reversible step of this reaction is believed to be largely dependent on the rate of dehydration of **I**.

*3.2. In vitro antiproliferative activities of novel 3-(4-nitrophenyl)-8-aryl-7,8-dihydroimidazo[2,1-c][1,2,4]triazin-4(6H)-ones (**10–18**)*

The designed and synthesized fused azaisocytosine-like congeners (**10–18**) were screened thoroughly for their *in vitro* antiproliferative effects (measured by BrdUrd incorporation) against a panel of five reference cell lines (A549, HeLa, T47D, TOV112D and Vero) of the same epithelial origin. An efficient, reliable and reproducible BrdUrd-ELISA method is a derivative of the traditional radioactive [^{3}H]-thymidine incorporation assay. The main advantage of this approach is that it permits a quantitative estimate of the incorporation of the labelled nucleoside analogue (as the fraudulent thymidine precursor) without the possibility of working with radioactive isotopes (Sztanke et al., 2015). The employed assay is commonly accepted in the preliminary phase of the discovery process directed towards development of novel anticancer agents (Vega-Avila and Pugsley, 2011). The BrdUrd-based method proved to be as sensitive as [^{3}H]-thymidine assay in previous *in vitro* investigations (Muir et al., 1990; Hawker, 2003). According to the manufacturer's protocol the results obtained with these two assays are strongly correlated together.

Table 1 specifies the percentage growth inhibition ratio of both tumour and normal cells by the 50 μg mL^{-1} concentration of all fused azaisocytosine-like congeners (**10–18**) after 24-, 48- and 72-h periods of incubation. Table 2 lists the IC_{50} values (the half maximal inhibitory concentrations calculated from the concentration-dependent inhibition curves) for the examined compounds.

All novel 3-(4-nitrophenyl)-8-aryl-7,8-dihydroimidazo[2,1-*c*][1,2,4]triazin-4(6*H*)-ones (**10–18**) exerted a cytotoxic effect in the majority of recruited tumour cells. It should be noted that all molecules at an effective concentration (50 μg mL^{-1}) revealed significantly higher antiproliferative effects in three malignant cells (A549, HeLa and T47D) than those evoked by the 100 μg mL^{-1} concentration of commonly used folate antimetabolite – pemetrexed (Sztanke et al., 2015). Pemetrexed

Please cite this article in press as: Sztanke, M. et al., Synthesis, structure elucidation, determination of antiproliferative activities, lipophilicity indices and pharmacokinetic properties of novel fused azaisocytosine-like congeners. Arabian Journal of Chemistry (2016), http://dx.doi.org/10.1016/j.arabjc.2016.04.002

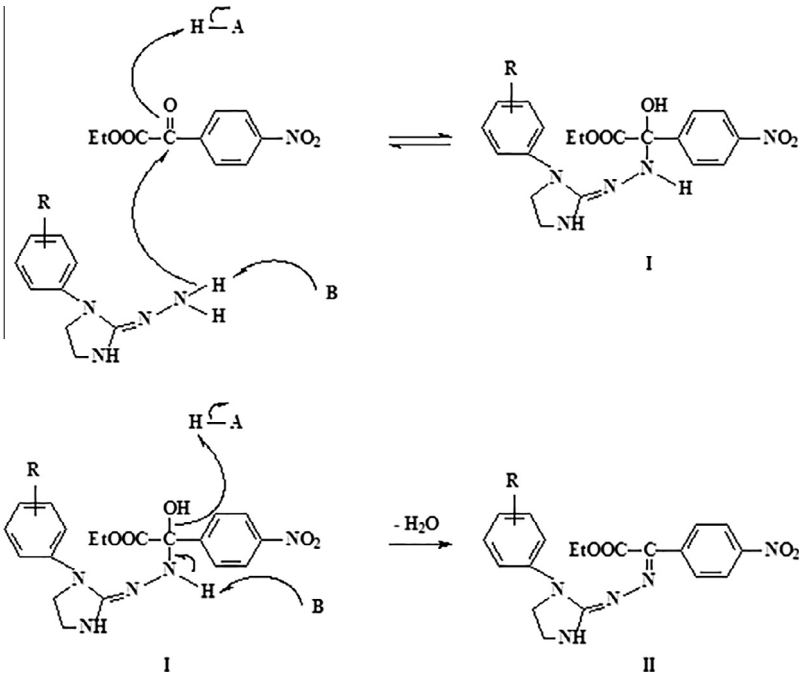

Scheme 2 The proposed stepwise mechanism for the formation of ketimine-type Schiff bases (**II**).

was employed in our studies as a standard drug, since this congener of folic acid is clinically used in patients suffering from non-small cell lung cancer. The inhibition of proliferation of tumour cells by the investigated congeners having incorporated fused azaisocytosine template is thought to be due to competition for nucleotides required for DNA biosynthesis (Rusinov et al., 2008).

Analysing the antiproliferative activities of the target fused azaisocytosine-containing congeners with the phenyl, alkylphenyl, dialkylphenyl and alkoxyphenyl substitution pattern at the *N*-8 (**10–14**) it has been noticed that the parent compound (**10**), with an electron-rich phenyl ring, is more cytotoxic for T47D, A549 and TOV112D cells than are either its substituted derivatives. However, the most promising compounds seemed to be **12** and **14** (bearing the electron-donating *para*-CH_3 and *ortho*-CH_3O group, respectively, at the phenyl ring) because they possess the highest cytotoxic activity against HeLa cells, displaying only a slight toxicity on normal cells after a 24-h incubation period.

Amongst the compounds bearing the mono- and dichlorophenyl substitution at the *N*-8 of the template (**15–18**), the derivatives **16**, **17** and **18** (that have electron-withdrawing groups attached at *meta*-Cl, *para*-Cl and 3,4-Cl_2 position, respectively, of the phenyl ring) were chosen as capable of producing the highest cytotoxic effects in T47D cells. The highest antiproliferative activities in TOV112D cells were achieved by introducing the 4-Cl and 3,4-Cl_2 group at the phenyl ring (compounds **17** and **18**, respectively), whereas in A549 cells – *via* the 3-Cl and 3,4-Cl_2 substitution (compounds **16** and **18**, respectively). The derivative **15** with the Cl group at an *ortho* position on the phenyl moiety, although displaying cytotoxic effects in tumour cells, proved to be the lowest toxic for normal cells in the series of chloro-substituted congeners, particularly when investigated after 24 and 48 h of incubation. Moving the Cl group to the *meta* position of the phenyl ring resulted in still antiproliferative active compound **16** (against T47D and TOV112D cells), with an increased cytotoxicity for A549 and HeLa cells after 24 and 48 h of incubation, respectively, when compared to **15**. Almost none of the enhancement in the antiproliferative activity against tumour cells was attained by introducing the chlorine atom into the position *para* of the phenyl ring, as proved for **17** when compared to **16**. In the case of the antiproliferative active compound with the 3-Cl substitution (**16**), introducing a further Cl substituent at position *para* of the phenyl moiety resulted in still antiproliferative active 3,4-Cl_2 substituted molecule (**18**), although revealing the decreased cytotoxicity for normal cells after 24- and 48-h incubation periods.

The bioisosteric replacements of the CH_3 group (susceptible to oxidation *in vivo* (Patrick, 2009)) that is placed both in the *ortho* and in the *para* position of the phenyl ring (compounds **11** and **12**, respectively) with a Cl group (resistant to oxidative biotransformation *in vivo* (Patrick, 2009)) led to *in vitro* antiproliferative active bioisosteres (molecules **15** and **17**, respectively). The best balance of cytotoxicity versus more selectivity was achieved by introducing a Cl group (compound **15**) in the case of the *ortho*-substituted isosteres (**11** and **15**) or a CH_3 group (compound **12**) in the case of *para*-substituted isosteres (**12** and **17**).

Introducing the methoxy group at the *ortho* position of the phenyl ring turned out to be the successful structural modification leading to a decrease in the cytotoxicity towards normal cells, which was particularly seen after 24 and 48 h of incubation as confirmed in the case of the compound **14**, when compared to the parent structure (**10**).

Placing a methyl group *ortho* to the phenyl ring led to a decrease in cytotoxicity towards normal cells only after 48- and 72-h incubation periods, as confirmed in the case of the structure **11** (when compared to **10**). Introducing a further methyl group to the phenyl ring resulted in a decrease of toxic

Please cite this article in press as: Sztanke, M. et al., Synthesis, structure elucidation, determination of antiproliferative activities, lipophilicity indices and pharmacokinetic properties of novel fused azaisocytosine-like congeners. Arabian Journal of Chemistry (2016), http://dx.doi.org/10.1016/j.arabjc.2016.04.002

Table 2 The IC_{50} values for all novel fused azaisocytosine-like congeners.

Compound	Incubation time	IC_{50} values (mM)[a]				
		Vero	A549	HeLa	T47D	TOV112D
10	24 h	>0.15	0.11 ± 0.011	0.09 ± 0.009	0.08 ± 0.010	0.09 ± 0.009
	48 h	0.08 ± 0.009	0.08 ± 0.008	0.08 ± 0.009	0.08 ± 0.008	0.08 ± 0.010
	72 h	0.08 ± 0.012	0.08 ± 0.010	0.08 ± 0.008	0.08 ± 0.008	0.08 ± 0.008
11	24 h	0.14 ± 0.018	0.10 ± 0.011	0.09 ± 0.009	0.12 ± 0.012	0.09 ± 0.007
	48 h	0.10 ± 0.007	0.09 ± 0.009	0.08 ± 0.009	0.09 ± 0.009	0.08 ± 0.007
	72 h	0.08 ± 0.008	0.07 ± 0.008	0.07 ± 0.009	0.08 ± 0.008	0.07 ± 0.007
12	24 h	>0.14	>0.14	0.08 ± 0.008	0.08 ± 0.009	0.09 ± 0.007
	48 h	0.09 ± 0.008	0.14 ± 0.016	0.08 ± 0.008	0.07 ± 0.007	0.08 ± 0.005
	72 h	0.07 ± 0.011	0.09 ± 0.009	0.07 ± 0.007	0.07 ± 0.008	0.08 ± 0.006
13	24 h	>0.14	>0.14	0.09 ± 0.008	0.09 ± 0.009	0.14 ± 0.010
	48 h	0.14 ± 0.011	0.09 ± 0.010	0.08 ± 0.008	0.07 ± 0.006	0.08 ± 0.006
	72 h	0.08 ± 0.011	0.08 ± 0.008	0.08 ± 0.008	0.07 ± 0.008	0.07 ± 0.008
14	24 h	>0.14	>0.14	0.08 ± 0.007	0.09 ± 0.008	0.09 ± 0.008
	48 h	>0.14	0.09 ± 0.010	0.08 ± 0.009	0.08 ± 0.007	0.08 ± 0.008
	72 h	0.09 ± 0.006	0.09 ± 0.010	0.07 ± 0.007	0.07 ± 0.007	0.07 ± 0.007
15	24 h	>0.14	0.14 ± 0.013	0.10 ± 0.009	0.08 ± 0.006	0.08 ± 0.006
	48 h	0.14 ± 0.016	0.08 ± 0.008	0.08 ± 0.008	0.07 ± 0.006	0.07 ± 0.007
	72 h	0.08 ± 0.008	0.07 ± 0.008	0.07 ± 0.008	0.07 ± 0.006	0.07 ± 0.008
16	24 h	0.09 ± 0.008	0.08 ± 0.008	0.08 ± 0.007	0.07 ± 0.004	0.08 ± 0.007
	48 h	0.08 ± 0.007	0.07 ± 0.008	0.07 ± 0.007	0.07 ± 0.006	0.07 ± 0.006
	72 h	0.07 ± 0.006	0.07 ± 0.007	0.07 ± 0.008	0.07 ± 0.007	0.07 ± 0.007
17	24 h	0.14 ± 0.013	0.09 ± 0.008	0.08 ± 0.008	0.07 ± 0.006	0.08 ± 0.006
	48 h	0.07 ± 0.007	0.07 ± 0.007	0.08 ± 0.008	0.07 ± 0.008	0.07 ± 0.006
	72 h	0.07 ± 0.008	0.07 ± 0.007	0.07 ± 0.007	0.07 ± 0.007	0.07 ± 0.006
18	24 h	>0.12	0.08 ± 0.008	0.07 ± 0.006	0.07 ± 0.005	0.07 ± 0.006
	48 h	0.09 ± 0.010	0.06 ± 0.007	0.06 ± 0.005	0.06 ± 0.005	0.06 ± 0.006
	72 h	0.06 ± 0.008	0.06 ± 0.007	0.06 ± 0.006	0.06 ± 0.008	0.06 ± 0.005

[a] Each value is the mean ± standard deviation.

effects of the derivative **13** for normal cells mostly after 24 and 48 h of incubation, when compared to **11**. Placing a methyl group *para* to the phenyl ring led to a decrease in cytotoxicity against normal cells after 24- and 48-h incubation periods, as confirmed in the case of the molecule **12** (when compared to **10**).

Experimental results proved that the attachment of mostly electron-donating moieties such as 4-CH_3, 2,3-$(CH_3)_2$, 2-CH_3O and electron-withdrawing 2-Cl and 3,4-Cl_2 groups at the phenyl ring, enhanced the selectivity for malignant over normal cells of the compounds **12**, **13**, **14**, **15** and **18** after 24 h of their incubation. However, they showed rather little selectivity after 48- and 72-h incubation periods.

*3.3. Assessment of the drug-likeness of the investigated fused azaisocytosine-containing congeners (**10–18**)*

According to the Lipinski's rule of five (Lipinski et al., 2001), all the reported in this study unknown congeners (**10–18**) have the increased chances of good oral bioavailability by the reason of fact that they have the following: the calculated log *P* values less than 5 and the overall molecular weights below 500 Da, not more than 5 H-bond donor and 10 H-bond acceptor sites. Furthermore, the analyzed compounds predicted to be conformationally stable as their molecules have less than 10 rotatable bonds, whereas their topological polar surface areas are less than 140 $Å^2$. These predictable molecular descriptors, shown in Table S1 in Supplementary material, were in the optimum range as that reported for the orally and intestinally bioavailable pharmaceutics (Veber et al., 2002; Eartl et al., 2000; Palm et al., 1997).

*3.4. Chromatographic behaviour and the individual retention factors of novel solutes (**10–18**)*

The chromatographic behaviour of this novel class of the compounds (**10–18**) was established. The isocratic retention factors, logs *k* (Yamagami et al., 1990, 1994; Klein et al., 1988), were measured directly by reversed phase liquid chromatography (RPLC) on three different columns in 20 °C (293 K) as well as 37 °C (310 K). Chromatographic analyses were carried out using buffered aqueous eluent systems containing as an organic modifier 40% (v/v) ($\log k_{0.4\ MeCN}$) and 50% (v/v) acetonitrile ($\log k_{0.5\ MeCN}$). An immobilized artificial membrane (IAM), an immobilized cholesterol (that imitate biological systems) and an internal surface reversal phase (ISRP), respectively, were employed as three different stationary materials. The choice of the endcapped stationary phases was aimed at

minimizing secondary retention mechanisms. It is well known that HPLC columns without endcapping have significant amounts of silanol groups capable of secondary silanophilic interactions which interfere with the partitioning mechanism. This is especially noticeable when employing acetonitrile as the mobile phase component.

The primary advantages of the performed direct RPLC measurements should be underlined. The retention parameters, logs k, were employed as the descriptors of lipophilicity. Thus this allowed not only to significantly shorten the retention times of compounds under study but also significantly reduce the overall time and costs of RPLC measurements that were carried out. It should be noted that the reliable and reproducible logs k of the compounds of interest are different flavours of their lipophilicity. All these isocratic retention factors that are the first time presented will be indispensable in further bioactivity predictions.

The correlation matrix concerning the results obtained on three different columns is listed in Table S2 in Supplementary material. The plot correlating log $k_{0.4\ MeCN,\ 310K}$ and log $k_{0.4\ MeCN,\ 293K}$ values measured on three different stationary phases is presented in Fig. S1A in Supplementary material. On the other hand, the plot of logs $k_{0.5\ MeCN,\ 310K}$ versus logs $k_{0.5\ MeCN,\ 293K}$ is shown in Fig. S1B in Supplementary material. The obtained results showed the column with an immobilized cholesterol is the most selective in relation to the analyzed compounds because their experimental logs k are the most varied. Furthermore, it has been shown that a bit weaker selectivity to the analyzed solutes reveals the IAM column, whereas the ISRP column seems to be the distinctly less selective for these types of analytes as their determined log k factors are the least varied.

It has been shown that the structure-dependent lipophilic properties of the individual compounds have a remarkable influence on their chromatographic behaviour and retention factors (Table 3). This is, as expected, taking into account the background theory of retention explaining that in the RPLC measurements the retention is governed by hydrophobic forces and therefore the lipophilicity of the individual solute is governing the retention (Cimpan et al., 2000; Dill and Dorsey, 1994; Dorsey et al., 1989; Dorsey and Khaledi, 1993; Valko, 2004; Gocan and Cimpan, 2006; Kaliszan, 2007). It is obvious that the structure-retention behaviour of solutes in reversed phase chromatographic investigations (that are of dynamic nature) determinates their fundamental processes of pharmacokinetic phase, e.g., liberation, absorption, distribution, metabolism and elimination (LADME) that occur in a living organism (Dorsey and Khaledi, 1993; Kaliszan, 2007; Perisic-Janjic et al., 2011; Janicka et al., 2013).

The combined electronic effects of the groups within the molecules investigated and resulting steric interactions may have influence on their determined log k parameters (Table 3). It seems that these ones although in part were capable of significantly perturbing the reported earlier hydrophobicity constant increment of some substituents attached to the aromatic systems (Hansch and Leo, 1979; Fujita et al., 1964).

Effects of a number of electron-donating and electron-withdrawing substituents attached at the phenyl moiety on decreasing and increasing logs k were thoroughly investigated. The parent compound (**10**) has a non-substituted electron-rich phenyl as the first aromatic moiety attached at the *N*-8 of the common template and the electron-withdrawing *para*-NO_2 group at the second phenyl ring. All the solutes **11–14** possess electron-donating substituents located at the first phenyl ring in different positions and additionally the electron-withdrawing NO_2 group in the *para* position at the second phenyl moiety. In turn, all the compounds **15–18** have electron-withdrawing substituents located at the first phenyl ring in different positions as well as the electron-withdrawing NO_2 group in the *para* position at the second phenyl moiety. It has been confirmed that electron-donating substituents located on the phenyl moiety decreased the logs k of the investigated compounds in the order: 2-CH_3 > 2-CH_3O > 4-CH_3 > 2,3-$(CH_3)_2$, when the RPLC measurements were carried out on the cholesterol column at both temperatures and both acetonitrile volume concentrations as well as on the IAM column at 20 °C using 50% acetonitrile in the mobile phase. In turn, the log k parameters of the same compounds decreased in the order of 2-CH_3 > 2-CH_3O > 2,3-$(CH_3)_2$ > 4-CH_3, when the chromatographic measurements were performed on the IAM column at 37 °C employing 40% acetonitrile in the mobile phase, on the IAM column at both temperatures employing 50% acetonitrile and on the ISRP column at both temperatures and both acetonitrile volume concentrations. Furthermore, it has been observed that electron-withdrawing substituents attached at the phenyl moiety decreased the log k factors of the studied solutes in the order: 3,4-Cl_2 > 4-Cl > 2-Cl > 3-Cl, when the chromatographic measurements were carried out at both temperatures on the column with an immobilized cholesterol as the stationary phase employing both acetonitrile volume concentrations, on the IAM column using 50% acetonitrile in the mobile phase and on the ISRP column employing 40% acetonitrile. In turn, the logs k of the same compounds decreased in the order of 3,4-Cl_2 > 4-Cl > 3-Cl > 2-Cl, when the chromatographic measurements were performed at both temperatures on the IAM column employing 40% acetonitrile in the mobile phase and on the ISRP column using 50% acetonitrile.

Introducing two electron-donating methyl groups to the parent molecule (**10**) resulted in a noticeable decrease of the determined logs k of the 2,3-$(CH_3)_2$-substituted compound (**18**). The most probable explanation would account for the steric hindrance of the modified molecule, which decreased its lipophilicity. Generally, it has been confirmed that the log k factors of the positional isomer with the *para*-Cl substitution (**17**) are higher than those of the *ortho*-Cl and *meta*-Cl substituted isomers (**15** and **16**, respectively). Introducing the second chlorine atom to the *para*-Cl and *meta*-Cl derivatives (**16** and **17**, respectively) evoked an increase in the log k parameters of the 3,4-Cl_2-substituted solute (**18**). Additionally, the determined retention factors of the *ortho*-substituted compounds proved to be distinctly lower than those predicted by an ACD/Percepta software. The decreasing and increasing experimental log k values of the molecules with an *ortho* substitution at the phenyl ring can be explained by taking into account the ortho effect. The most probable hypothesis is that 2,3-$(CH_3)_2$ and 2-Cl substituents in the *ortho* position caused the steric hindrance forcing-out-of-plane free rotation, whereas 2-CH_3 and 2-CH_3O groups were engaged in internal H-bond interactions (Hsieh and Dorsey, 1993; Van de Waterbeemd et al.,

Please cite this article in press as: Sztanke, M. et al., Synthesis, structure elucidation, determination of antiproliferative activities, lipophilicity indices and pharmacokinetic properties of novel fused azaisocytosine-like congeners. Arabian Journal of Chemistry (2016), http://dx.doi.org/10.1016/j.arabjc.2016.04.002

Table 3 The *in silico* molecular descriptors that are related to pharmacokinetics, retention factors (logs k) measured directly for a given system and calculated partition coefficients (expressed as logs P) of the compounds investigated.

Compound	10	11	12	13	14	15	16	17	18
log BB $_{distribution}$	−0.059	0.133	0.133	0.32	−0.086	0.049	0.102	0.038	0.183
$f_{u\ plasma}$	0.02	0.02	0.02	0.019	0.021	0.011	0.011	0.014	0.007
log BB $_{permeation}$	−1.11	−0.96	−0.96	−0.77	−0.93	−1.01	−1.12	−1.15	−1.13
log K_{HSA}	5.1	5.16	5.16	5.18	5.17	5.42	5.4	5.38	5.75
% F	77	62	62	53	71	27	26	18	5
$P_{e,\ jejunum} \times 10^4$ [cm s^{-1}]	7.96	7.84	7.84	7.71	7.73	7.87	7.87	7.85	7.75
Caco-2 $\times 10^6$ [cm s^{-1}]	223	232	232	238	218	236	236	230	241
log P	2.311	2.928	2.928	3.54	2.303	2.81	2.995	2.786	3.478
log $k_{IAM,\ 0.4\ MeCN,\ 293\ K}$	0.091	0.402	−0.139	−0.086	0.18	−0.033	−0.043	0.364	0.661
log $k_{IAM,\ 0.5\ MeCN,\ 293\ K}$	−0.319	−0.114	−0.541	−0.55	−0.284	−0.469	−0.463	−0.118	0.097
log $k_{IAM,\ 0.4\ MeCN,\ 310\ K}$	0.138	0.448	−0.075	−0.041	0.241	0.024	0.047	0.412	0.709
log $k_{IAM,\ 0.5\ MeCN,\ 310\ K}$	−0.252	−0.059	−0.419	−0.369	−0.198	−0.366	−0.343	−0.094	0.119
log $k_{Cholester,\ 0.4\ MeCN,\ 293\ K}$	1.055	1.441	0.804	0.746	1.283	0.991	0.872	1.456	1.792
log $k_{Cholester,\ 0.5\ MeCN,\ 293\ K}$	0.651	0.949	0.437	0.391	0.829	0.58	0.491	0.968	1.225
log $k_{Cholester,\ 0.4\ MeCN,\ 310\ K}$	1.009	1.374	0.766	0.738	1.214	0.952	0.831	1.372	1.704
log $k_{Cholester,\ 0.5\ MeCN,\ 310\ K}$	0.591	0.888	0.392	0.369	0.769	0.534	0.443	0.897	1.154
log $k_{ISRP,\ 0.4\ MeCN,\ 293\ K}$	−0.003	0.111	−0.058	−0.028	0.036	−0.014	−0.012	0.099	0.179
log $k_{ISRP,\ 0.5\ MeCN,\ 293\ K}$	−0.1	−0.046	−0.143	−0.134	−0.087	−0.118	−0.117	−0.047	0.002
log $k_{ISRP,\ 0.4\ MeCN,\ 310\ K}$	−0.084	0.016	−0.144	−0.12	0.072	−0.111	−0.114	0.02	0.148
log $k_{ISRP,\ 0.5\ MeCN,\ 310\ K}$	−0.316	−0.265	−0.351	−0.33	−0.321	−0.337	−0.324	−0.277	−0.229

log BB $_{distribution}$ – distribution of the solute between the blood–brain; $f_{u,\ plasma}$ – fraction unbound of the solute in the plasma; log BB $_{permeation}$ – permeation of the solute through the blood–brain barrier; log K_{HSA} – binding of the compound with human albumin serum and controlling the fraction unbound in body compartments in equilibrium with the plasma;%F – oral bioavailability of the solute after per os administration at a dose of 50 mg; $P_{e,\ jejunum}$ – human jejunal score (pH 6.5); Caco-2 permeability value – is employed for assessing the intestinal absorption; log P – the calculated logarithms of *n*-octanol-water coefficients; log $k_{IAM,\ 0.4\ MeCN,\ 293K}$ – the retention factors, log k obtained on the immobilized artificial membrane (IAM)-type column with buffer-acetonitrile 0.4 v/v mobile phases at 20 °C (293 K); log $k_{IAM,\ 0.5\ MeCN,\ 293K}$ – the retention factors, log k obtained on the IAM-type column with buffer-acetonitrile 0.5 v/v mobile phases at 20 °C (293 K); log $k_{IAM,\ 0.4\ MeCN,\ 310K}$ – the retention factors, log k obtained on the IAM-type column with buffer-acetonitrile 0.4 v/v mobile phases at 37 °C (293 K); log $k_{IAM,\ 0.5\ MeCN,\ 310K}$ – the retention factors, log k obtained on the IAM-type column with buffer-acetonitrile 0.5 v/v mobile phases at 37 °C (293 K); log $k_{Cholester,\ 0.4\ MeCN,\ 293K}$ – the retention factors, log k obtained on the column with an immobilized cholesterol, as the stationary phase with buffer-acetonitrile 0.4 v/v mobile phases at 20 °C (293 K); log $k_{Cholester,\ 0.5\ MeCN,\ 293K}$ – the retention factors, log k obtained on the column with an immobilized cholesterol, as the stationary phase with buffer-acetonitrile 0.5 v/v mobile phases at 20 °C (293 K); log $k_{Cholester,\ 0.4\ MeCN,\ 310K}$ – the retention factors, log k obtained on the column with an immobilized cholesterol, as the stationary phase with buffer-acetonitrile 0.4 v/v mobile phases at 37 °C (310 K); log $k_{Cholester,\ 0.5\ MeCN,\ 310K}$ – the retention factors, log k obtained on the column with an immobilized cholesterol, as the stationary phase with buffer-acetonitrile 0.5 v/v mobile phases at 37 °C (310 K); log $k_{ISRP,\ 0.4\ MeCN,\ 293K}$ – the retention factors, log k obtained on the ISRP-type column with buffer-acetonitrile 0.4 v/v mobile phases at 20 °C (293 K); log $k_{ISRP,\ 0.5\ MeCN,\ 293K}$ – the retention factors, log k obtained on the ISRP-type column with buffer-acetonitrile 0.5 v/v mobile phases at 20 °C (293 K); log $k_{ISRP,\ 0.4\ MeCN,\ 310K}$ – the retention factors, log k obtained on the ISRP-type column with buffer-acetonitrile 0.4 v/v mobile phases at 37 °C (310 K); log $k_{ISRP,\ 0.5\ MeCN,\ 310K}$ – the retention factors, log k obtained on the ISRP-type column with buffer-acetonitrile 0.5 v/v mobile phases at 37 °C (310 K).

1996; Lambert, 1993; Carrupt et al., 1997). This could be the cause why in our measurements 2,3-$(CH_3)_2$ and 2-Cl substituted molecules revealed decreased, whereas 2-CH_3 and 2-CH_3O ones had increased retention factors in relation to the parent structure (**10**).

3.5. Chromatographic retention factors versus partitioning lipophilicities

The relationships between computed log P values (by using an ACD/Percepta software) and experimentally obtained log k factors were carefully investigated.

Logs P versus logs k dependences were found to be explicitly linear for five compounds (**10**, **11**, **14**, **17** and **18**) of nine investigated (Fig. 2). The remaining four solutes (**12**, **13**, **15** and **16**), as typical outliers, had to be excluded from the regression equation. These outliers, although revealing the explicitly overestimated log P values in *in silico* calculations, proved to be distinctly less lipophilic in the empirical RPLC measurements. The same figure also shows that in the case of these outliers there are significant objections against their calculated lipophilicity indices. This means that the prediction of reliable log P values of molecules **12**, **13**, **15** and **16** is impossible and there is a clear need to verify the computed results experimentally.

Statistics of the relationships obtained by plotting log P versus log k values is presented in Table 4. The statistically significant very strong linear correlations were disclosed between the logarithms of predicted 1-octanol/water coefficients (expressed as log P values) and the logarithms of chromatographic retention parameters (expressed as the isocratic log k factors) measured on IAM (R^2 from 0.9684 to 0.9847; $p < 0.003$) and ISRP (R^2 from 0.9492 to 0.9923; $p < 0.005$) columns. Logs P versus logs k correlations proved to be also strong (R^2 from 0.8895 to 0.9056) and statistically significant ($p < 0.002$) when chromatographic measurements were

Please cite this article in press as: Sztanke, M. et al., Synthesis, structure elucidation, determination of antiproliferative activities, lipophilicity indices and pharmacokinetic properties of novel fused azaisocytosine-like congeners. Arabian Journal of Chemistry (2016), http://dx.doi.org/10.1016/j.arabjc.2016.04.002

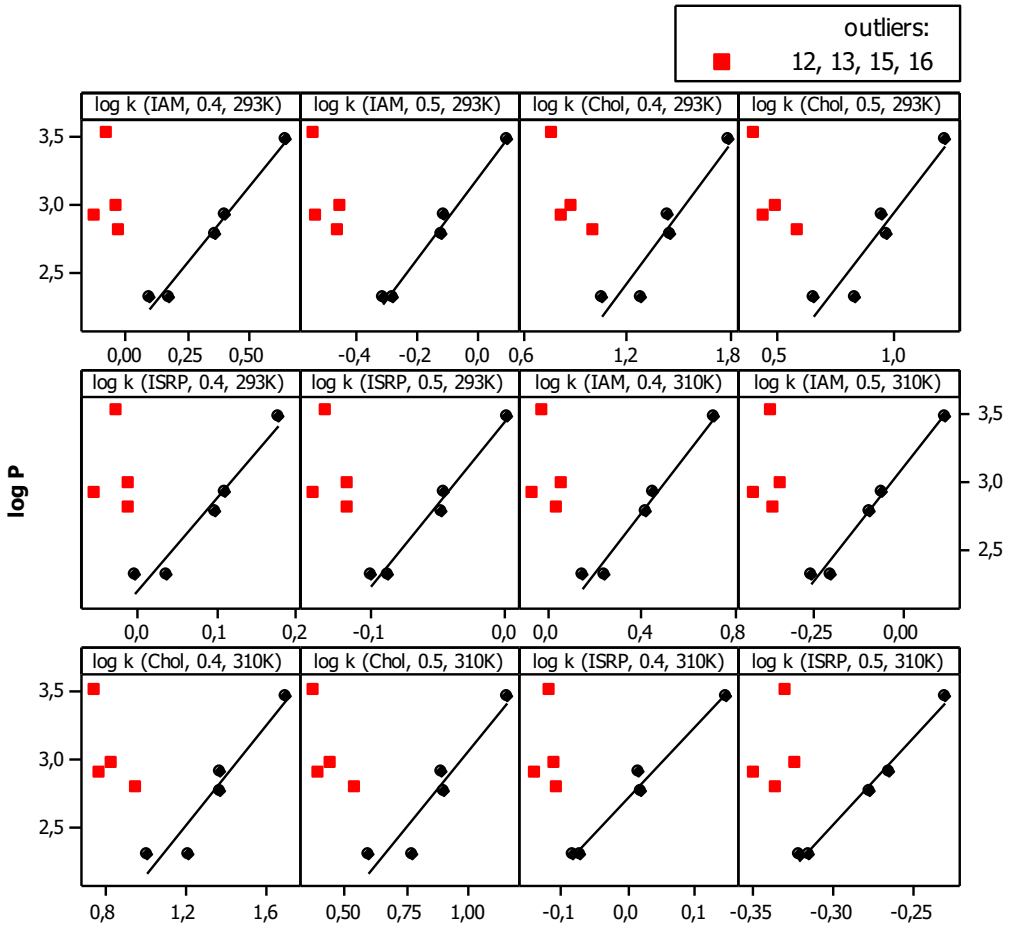

Figure 2 Log *P* versus log *k* relationships obtained for different HPLC systems at two temperatures (20 °C (293 K) and 37 °C (310 K)).

Table 4 Statistics of the relationships obtained by plotting logs *P* versus logs *k* (determined on three columns with different reversed-phase materials).

Stationary phase	φ_{MeCN}	Temperature (K)	$a \pm SE$	$b \pm SE$	S	R^2	F	p	n	Outliers
Equation: log P vs. log k: y = a (±SE) x + b (±SE)										
IAM	0.4	293	2.186 ± 0.196	2.019 ± 0.077	0.087	0.9763	124	0.0016	5	12, 13, 15, 16
		310	2.199 ± 0.229	1.905 ± 0.100	0.100	0.9684	92	0.0024	5	12, 13, 15, 16
	0.5	293	2.926 ± 0.211	3.193 ± 0.044	0.070	0.9847	193	0.0008	5	12, 13, 15, 16
		310	1.522 ± 0.052	3.087 ± 0.047	0.084	0.9781	134	0.0014	5	12, 13, 15, 16
Cholester	0.4	293	1.712 ± 0.342	0.356 ± 0.488	0.185	0.8929	26	0.0154	5	12, 13, 15, 16
		310	1.834 ± 0.340	0.327 ± 0.460	0.173	0.9056	29	0.0127	5	12, 13, 15, 16
	0.5	293	2.193 ± 0.446	0.734 ± 0.421	0.187	0.8896	25	0.0161	5	12, 13, 15, 16
		310	2.240 ± 0.456	0.835 ± 0.401	0.188	0.8895	25	0.0161	5	12, 13, 15, 16
ISRP	0.4	293	6.757 ± 0.903	2.191 ± 0.095	0.127	0.9492	57	0.0049	5	12, 13, 15, 16
		310	5.198 ± 0.428	2.732 ± 0.036	0.080	0.9801	148	0.0012	5	12, 13, 15, 16
	0.5	293	12.029 ± 1.089	3.430 ± 0.072	0.087	0.9760	123	0.0016	5	12, 13, 15, 16
		310	12.782 ± 0.651	6.361 ± 0.185	0.050	0.9923	386	0.0003	5	12, 13, 15, 16

Chromatographic parameters: $\varphi_{MeCN\ 0.4}$ and $\varphi_{MeCN\ 0.5}$ – indicate that mobile phases contained 0.4 ($\log k_{0.4}$) and 0.5 ($\log k_{0.5}$) volume fraction of acetonitrile (MeCN), respectively; Statistical terms for the derived regression equations: SE – denotes the standard error of regression coefficient, R^2 – is the square correlation coefficient, S – denotes the standard error of estimate, F – denotes the value of the Fischer's significance test, p – is the statistical significance level, n – denotes a number of the solutes involved in the derived regression equation.

performed on the column with an immobilized cholesterol as the stationary phase. This means that novel lipophilicity indices, giving a consistent scale of lipophilicity with the trustworthy partitioning descriptors (expressed as log *P* values) of the compounds **10**, **11**, **14**, **17** and **18**, may be regarded as their sustainable values of reference. However, the

computed log *P* values of solutes **12**, **13**, **15** and **16** cannot be used as the trustworthy descriptors of their lipophilicity, as confirmed above.

3.6. PCA

The principal component analysis-based approach was employed to visualize the systematic trends in existed similarities and dissimilarities between the chromatographic, partitioning and pharmacokinetic parameters characterizing fused azaisocytosine-like congeners of interest (**10–18**). The overall twenty data set variables including: the chromatographic retention factors (log $k_{\text{IAM 0.4, 293K}}$, log $k_{\text{IAM 0.5, 293K}}$, log $k_{\text{IAM 0.4, 310K}}$, log $k_{\text{IAM 0.5, 310K}}$, log $k_{\text{Cholester 0.4, 293K}}$, log $k_{\text{Cholester 0.5, 293K}}$, log $k_{\text{Cholester 0.4, 310K}}$, log $k_{\text{Cholester 0.5, 310K}}$, log $k_{\text{ISRP 0.4, 293K}}$, log $k_{\text{ISRP 0.5, 293K}}$, log $k_{\text{ISRP 0.4, 310K}}$, log $k_{\text{ISRP 0.5, 310K}}$), the predicted *n*-octanol/water partitioning parameters (expressed as log *P* values) and the *in silico* calculated molecular descriptors (log $BB_{\text{permeation}}$, log $BB_{\text{distribution}}$, log K_{HSA},%F, $f_{\text{u, plasma}}$, Caco-2, $P_{\text{e, jejunum}}$) that are relevant to pharmacokinetics of the investigated compounds were submitted to a rational PCA-based approach.

Three principal components explained 64.9%, 84.6% and 95.5% of the total variance, respectively. It should be noted that the results obtained by the principal component (see the loading plot presented in Fig. 3A) and cluster variables (see the dendrogram shown in Fig. 3B) analyses are consistent, confirming high trends in similarity between the analyzed chromatographic, partitioning and bioactivity parameters.

The loading plot (Fig. 3A) presents the relationships between all the variables after subjecting them to PCA. The majority of data set variables, including valuable bioactivity descriptors such as Caco-2, log K_{HSA}, log $BB_{\text{distribution}}$, all determined experimentally retention factors as well as the calculated partitioning coefficient logarithms, logs *P* proved to be similar to each other. In this case the *in silico* bioactivity descriptors were proportional to the retention parameters both determined experimentally and calculated *in silico*. All these data set variables formed an "acute arrow" on the right side of the chart. In turn, the other pharmacokinetic descriptor variables such as $P_{\text{e, jejunum}}$, %F, $f_{\text{u, plasma}}$, log $BB_{\text{permeation}}$ proved to be inversely proportional to the determined logarithms of retention factors as well as to the predicted logarithms of partition coefficients. All these data set variables formed an "acute arrow" on the left side of the chart.

Furthermore, the score plot (Fig. 3C) reveals the trends in similarities and dissimilarities between molecular structures of the compounds that were tested according to the chromatographic, partitioning and bioactivity variables. The investigated compounds have been divided into two separate clusters due to differences in their molecular structures. The first explicitly linear cluster is associated with five more lipophilic solutes (**10**, **11**, **14**, **17** and **18**) and the second cluster (with the scattered data points) is formed for four less lipophilic analytes (**12**, **13**, **15** and **16**). Such grouping of the tested solutes is most likely directly due to similarities in their retention mechanism (as evidenced by their logs *k*) obtained on different RPLC materials. The diverse grouping on the analyzed compounds may also suggest that the retention of each group of substances is controlled by the different net effect of intermolecular forces between the solute on subsequent reversed phase materials and the mobile phase (Kaliszan, 2007; Perisic-Janjic et al., 2011). It cannot be excluded that clustering of the compounds **12**, **13**, **15** and **16** may be presumably evoked by more complicated steric and electronic effects within their molecules that have a significant influence on their retention behaviour and consequently on bioactivity descriptors.

3.7. Correlations between chromatographic lipophilicity parameters and in silico calculated pharmacokinetic descriptors

The data sets of the determined retention factors (log *k*) on three different RPLC columns as well as *in silico* bioactivity descriptors (e.g.,%F, $f_{\text{u, plasma}}$, log K_{HSA}, log $BB_{\text{distribution}}$, log $BB_{\text{permeation}}$, Caco-2, $P_{\text{e, jejunum}}$) were correlated with the goal of evaluating whether the lipophilicity parameters have influence on the pharmacokinetic properties of our novel compounds. This approach was performed with the purpose of preselecting the lead candidates for further *in vivo* studies with optimum lipophilicity ranges relevant to satisfactory pharmacokinetics. Knowledge about pharmacokinetic properties of compounds with sufficient *in vitro* biological activities is especially important before subjecting them to further *in vivo* investigations. It is commonly known that poor pharmacokinetics, in the majority cases, results in drug candidate failure. Therefore, *in silico* predictive models are very helpful at an early discovery phase of new biologically active compounds that are considered as potential drug candidates (Guerra et al., 2010; Matysiak et al., 2015).

All the *in silico* calculated pharmacokinetic descriptors of the investigated solutes are listed in Table 3. %F value is used in an early phase of the lead candidate selection process for predicting the bioavailability of the solute after *per os* administration, whereas the $f_{\text{u, plasma}}$ predictor is used for assessing a fraction unbound of the compound of interest in the plasma (e.g., actually active). Log K_{HSA} value is employed for predicting the solute binding with human serum albumin as the most significant protein component. Caco-2 and $P_{\text{e, jejunum}}$ predictors are used for assessing the intestinal absorption and an effective transport in human jejunum, respectively. Log $BB_{\text{distribution}}$ value predicts the distribution of the individual solute between the blood–brain, whereas log $BB_{\text{permeation}}$ value predicts the ability of the solute to penetrate the blood–brain barrier.

Plots of the *in silico* pharmacokinetic descriptors against the experimental retention factors are shown in Fig. 4A–C and apart from that in Fig. S2 in Supplementary material. The described correlations between physico-chemical properties strictly related to pharmacokinetics and retention factors of the analyzed new compounds on different reversed phase stationary materials are presented in Table 5 and apart from that in Table S3 in Supplementary material. The determined log *k* factors proved to be applicable in predictions of some fundamental pharmacokinetic properties of the studied solutes such as%F, $f_{\text{u, plasma}}$, log K_{HSA} values.

Fig. 4A shows the relationships between the calculated oral bioavailability values (expressed as %F) and the experimental retention factors. These dependences are described by two quadratic equations that were found to be separated for solutes **15–18** and **10–14**. The statistically significant and very strong curvilinear relationships (R^2 in the range from 0.9979 to

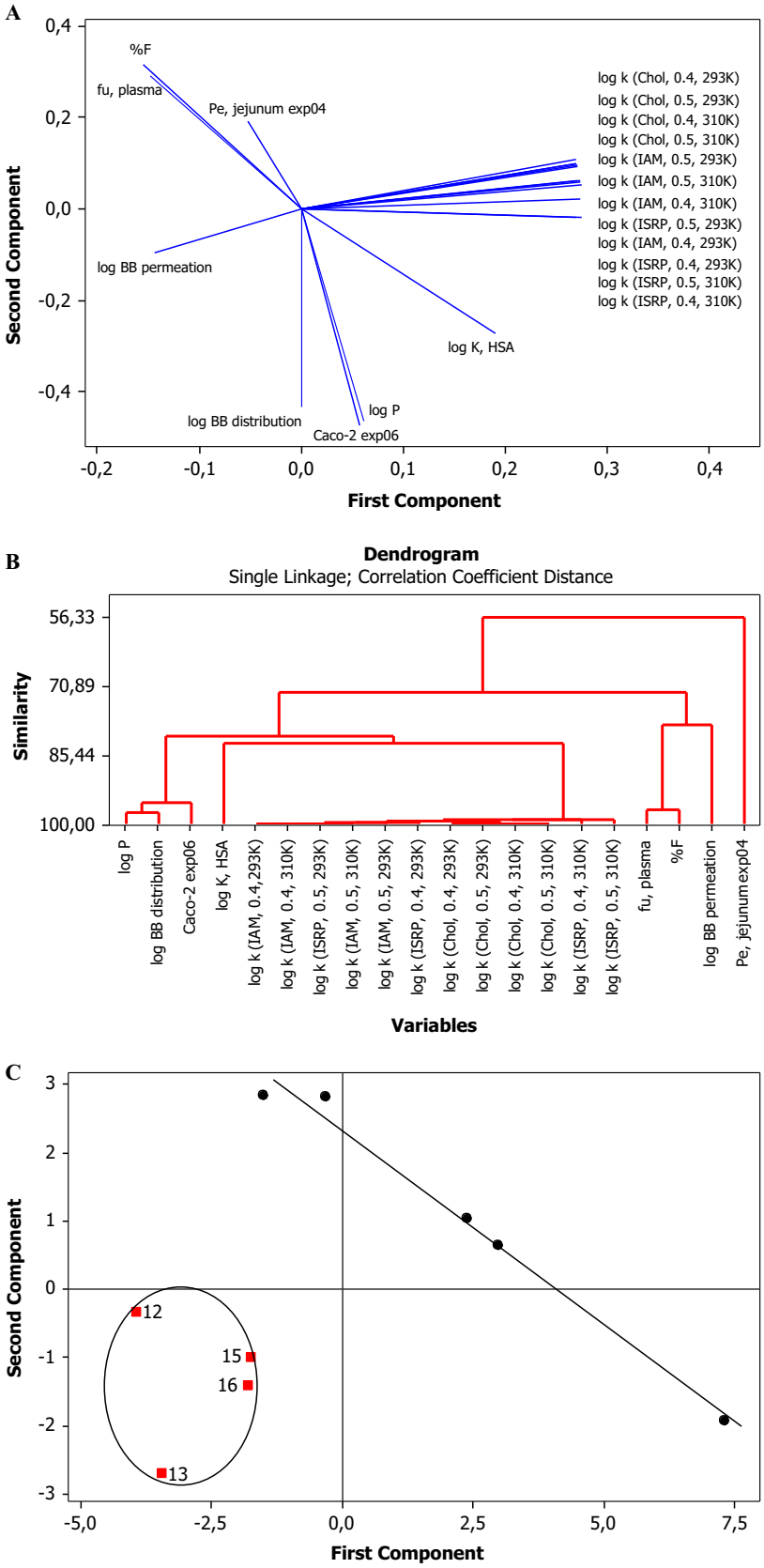

Figure 3 Loading plot (A), dendrogram (B) and score plot of *PC2* against *PC1* for the PCA-based approach (C).

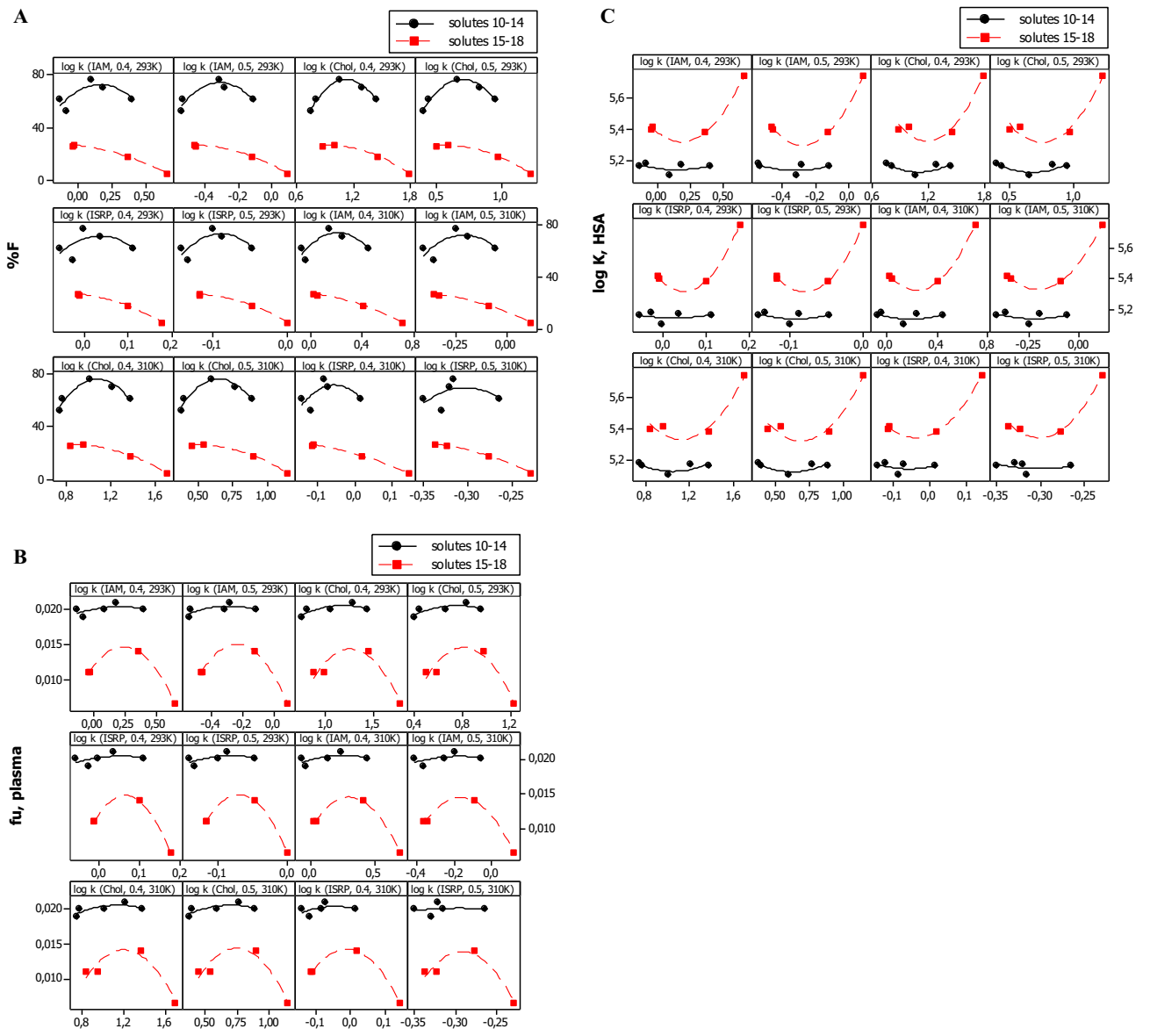

Figure 4 Relationships between pharmacokinetic descriptors and retention factors: (A) %F predictors versus log *k* factors; (B) $f_{\text{u plasma}}$ predictors versus log *k* factors; (C) log K_{HSA} predictors versus log *k* factors.

0.9999) were identified between the %F predictors and the log *k* factors of compounds **15–18** established on IAM and ISRP columns. %F versus logs *k* relationships were again very strong (R^2 in the range from 0.9965 to 0.9985) when the measurements were performed on the column with an immobilized cholesterol. The disclosed curvilinear shapes of these correlation lines indicate that an enhancement in the solutes' lipophilicities (expressed as logs *k*) reduces their bioavailability after *per os* administration. In turn, %F values of the compounds **10**–**14** plotted against the log *k* factors determined on the cholesterol column at the temperature of 20 °C revealed also statistically significant and very strong parabolic correlations (R^2 = 0.9746 and 0.9797).

Fig. 4B presents the relationships between the pharmacokinetically active fraction unbound in the plasma ($f_{\text{u, plasma}}$) and the determined experimentally retention factors. The parabolic shape of shown correlation lines suggests that there exists an optimum range of lipophilicity providing a proper binding of the solute in the plasma. The relationships between the $f_{\text{u, plasma}}$ predictors and the chromatographic retention parameters are described by quadratic equations for solutes **15–18**. The strongest and statistically significant correlations were identified by plotting $f_{\text{u, plasma}}$ predictors versus the log *k* factors obtained from measurements that were performed at 20 °C on IAM (R^2 = 0.9988 and 0.9992) and ISRP (R^2 = 0.9993 and 0.9996) columns. In turn, in the case of solutes revealing lower binding with plasma proteins and forming the separate group (**10–14**) no effect of the retention factors on their optimal binding with plasma was observed. All the tested substances (**10–18**) predicted to have a high protein binding behaviour (according to the known protein binding classification (Idaidek and Arafat, 2012; Amidon et al., 1995)) as their overall fraction unbound in human blood plasma is relatively low (< 0.1).

Table 5 Statistics of the relationships obtained by plotting the *in silico* molecular descriptors related to pharmacokinetics versus log *k* factors.

Stationary phase	φ_{MeCN}	Temperature (K)	$a \pm SE$	$b \pm SE$	$c \pm SE$	S	R^2	F	p	n	Compounds
Equation:%F vs. log k: $y = a (\pm SE)\ x^2 + b (\pm SE)\ x + c (\pm SE)$											
IAM	0.4	293	−185.079 ± 115.101	59.541 ± 34.709	68.142 ± 4.854	8.237	0.6032	1.6	0.3968	5	10–14
			−32.720 ± 7.617	−10.357 ± 4.599	26.143 ± 0.492	0.764	0.9981	266	0.0434	4	15–18
		310	−210.667 ± 110.859	88.434 ± 43.081	64.438 ± 4.190	7.417	0.6783	2.2	0.3217	5	10–14
			−30.843 ± 5.581	−8.968 ± 4.038	26.879 ± 0.447	0.529	0.9991	554	0.0300	4	15–18
	0.5	293	−317.289 ± 100.678	−199.729 ± 71.595	42.947 ± 10.846	4.799	0.8653	6.5	0.1347	5	10–14
			−63.608 ± 11.237	−61.658 ± 4.810	11.588 ± 0.528	0.698	0.9984	319	0.0396	4	15–18
		310	−380.403 ± 289.056	−163.568 ± 143.267	54.365 ± 15.185	9.093	0.5164	1.1	0.4836	5	10–14
			−58.538 ± 8.947	−59.214 ± 2.590	12.893 ± 0.351	0.424	0.9994	861	0.0241	4	15–18
Cholester	0.4	293	157.310 ± 19.866	353.779 ± 43.173	−12.074 ± 22.204	2.085	0.9746	38.4	0.0254	5	10–14
			−28.302 ± 5.262	51.960 ± 13.992	2.658 ± 8.649	0.853	0.9977	213	0.0484	4	15–18
		310	−178.776 ± 38.556	385.549 ± 80.506	−131.285 ± 39.935	3.494	0.9286	13.1	0.0714	5	10–14
			−39.502 ± 6.986	49.969 ± 17.710	5.377 ± 10.461	1.041	0.9965	143	0.0591	4	15–18
	0.5	293	−243.733 ± 27.723	338.998 ± 36.847	−41.001 ± 11.129	1.865	0.9797	48.2	0.0203	5	10–14
			−47.471 ± 6.741	52.225 ± 11.527	12.168 ± 4.392	0.679	0.9985	336	0.0386	4	15–18
		310	−274.359 ± 54.935	354.987 ± 68.146	−37.844 ± 19.147	3.254	0.9381	15.2	0.0619	5	10–14
			−48.180 ± 8.414	46.652 ± 13.416	15.215 ± 4.734	0.810	0.9979	236	0.0460	4	15–18
ISRP	0.4	293	−1545.96 ± 1593.22	110.460 ± 123.190	69.210 ± 6.690	10.665	0.3349	0.6	0.6651	5	10–14
			−448.029 ± 89.381	−37.608 ± 14.348	26.094 ± 0.432	0.671	0.9985	344	0.0381	4	15–18
		310	−1948.110 ± 1588.420	−211.860 ± 209.330	66.440 ± 4.480	9.736	0.4457	0.9	0.5543	5	10–14
			−145.628 ± 55.517	−77.354 ± 3.923	19.631 ± 0.791	0.802	0.9979	241	0.0456	4	15–18
	0.5	293	−5754.990 ± 3459.230	−1026.090 ± 669.050	27.200 ± 29.450	8.036	0.6224	1.7	0.3776	5	10–14
			−1204.700 ± 236.148	−319.00 ± 29.883	5.650 ± 0.645	0.682	0.9985	333	0.0387	4	15–18
		310	−5126.280 ± 6517.87	−3104.350 ± 3979.380	−399.850 ± 602.700	11.395	0.2407	0.4	0.7593	5	10–14
			−1129.230 ± 87.159	−844.040 ± 49.423	−129.090 ± 6.863	0.206	0.9999	366	0.0117	4	15–18
Equation: $f_{u,\ plasma}$ *vs. log k:* $y = a (\pm SE)\ x^2 + b (\pm SE)\ x + c (\pm SE)$											
IAM	0.4	293	−0.008 ± 0.011	0.003 ± 0.003	0.020 ± 0.001	0.001	0.3611	0.6	0.6389	5	10–14
			−0.047 ± 0.002	0.023 ± 0.001	0.01 ± 0.000	0.001	0.9988	417	0.0346	4	15–18
		310	−0.010 ± 0.011	0.005 ± 0.004	0.020 ± 0.000	0.001	0.4320	0.8	0.5680	5	10–14
			−0.049 ± 0.005	0.030 ± 0.003	0.010 ± 0.000	0.001	0.9936	78	0.0800	4	15–18
	0.5	293	−0.016 ± 0.014	−0.009 ± 0.010	0.019 ± 0.002	0.001	0.5409	1.2	0.4591	5	10–14
			−0.077 ± 0.002	−0.036 ± 0.001	0.011 ± 0.000	0.001	0.9992	633	0.0281	4	15–18
		310	−0.014 ± 0.027	−0.005 ± 0.013	0.020 ± 0.001	0.001	0.2831	0.4	0.7169	5	10–14
			−0.097 ± 0.013	−0.032 ± 0.004	0.012 ± 0.001	0.001	0.9876	40	0.1114	4	15–18
Cholester	0.4	293	−0.007 ± 0.006	0.016 ± 0.012	0.011 ± 0.006	0.001	0.6482	1.9	0.3518	5	10–14
			−0.028 ± 0.011	0.070 ± 0.028	−0.030 ± 0.017	0.002	0.8979	5	0.3195	4	15–18
		310	−0.008 ± 0.007	0.07 ± 0.015	0.011 ± 0.007	0.001	0.6008	1.6	0.3992	5	10–14
			−0.030 ± 0.012	0.071 ± 0.030	−0.029 ± 0.018	0.002	0.38929	5	0.3273	4	15–18
	0.5	293	−0.010 ± 0.009	0.015 ± 0.012	0.015 ± 0.004	0.001	0.6299	1.8	0.3701	5	10–14
			−0.045 ± 0.017	0.0725 ± 0.028	−0.015 ± 0.011	0.001	0.9018	5	0.3133	4	15–18
		310	−0.011 ± 0.011	0.015 ± 0.013	0.015 ± 0.004	0.001	0.5931	1.5	0.4069	5	10–14

(*continued on next page*)

Please cite this article in press as: Sztanke, M. et al., Synthesis, structure elucidation, determination of antiproliferative activities, lipophilicity indices and pharmacokinetic properties of novel fused azatisocytosine-like congeners. Arabian Journal of Chemistry (2016), http://dx.doi.org/10.1016/j.arabjc.2016.04.002

Table 5 (*continued*)

Stationary phase	φ_{MeCN}	Temperature (K)	$a \pm SE$	$b \pm SE$	$c \pm SE$	S	R^2	F	p	n	Compounds
			−0.046 ± 0.018	0.070 ± 0.028	−0.012 ± 0.010	0.002	0.9880	5	0.3193	4	15–18
ISRP	0.4	293	−0.071 ± 0.131	0.008 ± 0.010	0.020 ± 0.001	0.001	0.2338	0.4	0.7662	5	10–14
			−0.627 ± 0.018	0.081 ± 0.003	0.012 ± 0.000	0.001	0.9993	762	0.0256	4	15–18
		310	−0.090 ± 0.143	−0.008 ± 0.019	0.020 ± 0.001	0.001	0.2275	0.3	0.7725	5	10–14
			−0.311 ± 0.009	−0.006 ± 0.001	−0.014 ± 0.000	0.001	0.9994	780	0.0253	4	15–18
	0.5	293	−0.259 ± 0.343	−0.042 ± 0.066	0.019 ± 0.003	0.001	0.3626	0.6	0.6374	5	10–14
			−1.636 ± 0.039	−0.227 ± 0.005	0.007 ± 0.000	0.001	0.9996	1151	0.0208	4	15–18
		310	−0.121 ± 0.563	−0.072 ± 0.344	0.110 ± 0.052	0.001	0.0324	0.1	0.9676	5	10–14
			−1.839 ± 0.594	−1.074 ± 0.337	−0.143 ± 0.047	0.001	0.9312	7	0.2623	4	15–18
Equation: log K_{HSA} vs. log k: $y = a (\pm SE)\ x^2 + b (\pm SE)\ x + c (\pm SE)$											
IAM	0.4	293	0.396 ± 0.548	−0.114 ± 0.165	5.146 ± 0.023	0.039	0.2149	0.3	0.7851	5	10–14
			1.880 ± 0.200	−0.685 ± 0.121	5.381 ± 0.013	0.020	0.9957	116	0.0657	4	15–18
		310	0.467 ± 0.574	−0.176 ± 0.223	5.153 ± 0.022	0.038	0.2465	0.4	0.7535	5	10–14
			1.968 ± 0.009	−0.960 ± 0.006	5.441 ± 0.001	0.010	1.000	710	0.0027	4	15–18
	0.5	293	0.711 ± 0.749	0.456 ± 0.533	5.207 ± 0.081	0.036	0.3501	0.6	0.6499	5	10–14
			3.215 ± 0.146	1.790 ± 0.062	5.546 ± 0.007	0.009	0.9991	568	0.2967	4	15–18
		310	0.844 ± 1.264	0.383 ± 0.627	5.183 ± 0.066	0.040	0.1927	0.3	0.8073	5	10–14
			3.894 ± 0.089	1.636 ± 0.026	5.500 ± 0.003	0.004	0.9998	2626	0.0138	4	15–18
Cholester	0.4	293	0.435 ± 0.286	−0.952 ± 0.622	5.643 ± 0.320	0.030	0.5400	1.2	0.4600	5	10–14
			1.141 ± 0.431	−2.709 ± 1.147	6.931 ± 0.709	0.070	0.9474	9	0.2295	4	15–18
		310	0.478 ± 0.350	−1.006 ± 0.731	5.653 ± 0.362	0.032	0.4872	1.0	0.5128	5	10–14
			1.213 ± 0.466	−2.725 ± 1.182	6.862 ± 0.698	0.070	0.9479	10	0.2282	4	15–18
	0.5	293	0.694 ± 0.432	−0.932 ± 0.575	5.434 ± 0.174	0.029	0.5684	1.4	0.4316	5	10–14
			1.045 ± 0.235	−3.051 ± 0.777	6.130 ± 0.225	0.044	0.9789	24	0.1453	4	15–18
		310	0.763 ± 0.514	−0.952 ± 0.637	5.419 ± 0.179	0.030	0.5274	1.2	0.4726	5	10–14
			1.929 ± 0.729	−2.654 ± 1.163	6.234 ± 0.410	0.040	0.9468	9	0.2306	4	15–18
ISRP	0.4	293	2.583 ± 6.351	−0.131 ± 0.491	5.146 ± 0.027	0.043	0.0779	0.1	0.9331	5	10–14
			25.526 ± 1.295	−2.466 ± 0.208	5.374 ± 0.006	0.010	0.9990	490	0.0319	4	15–18
		310	3.749 ± 6.702	0.423 ± 0.883	5.153 ± 0.033	0.041	0.1390	0.2	0.8610	5	10–14
			11.920 ± 1.244	0.882 ± 0.088	5.358 ± 0.018	0.018	0.9965	143	0.0590	4	15–18
	0.5	293	12.335 ± 16.758	2.259 ± 3.244	5.241 ± 0.143	0.039	0.2255	0.3	0.7745	5	10–14
			66.847 ± 3.639	10.566 ± 0.461	5.729 ± 0.010	0.011	0.9998	420	0.0345	4	15–18
		310	11.824 ± 23.801	7.126 ± 14.531	6.215 ± 2.201	0.042	0.1166	0.2	0.8834	5	10–14
			76.139 ± 11.794	45.989 ± 6.688	12.286 ± 0.929	0.028	0.9916	60	0.0916	4	15–18

All statistical terms for the derived regression equations are explained underneath Table 5.

Please cite this article in press as: Sztanke, M. et al., Synthesis, structure elucidation, determination of antiproliferative activities, lipophilicity indices and pharmacokinetic properties of novel fused azaisocytosine-like congeners. Arabian Journal of Chemistry (2016), http://dx.doi.org/10.1016/j.arabjc.2016.04.002

Fig. 4C also shows plots correlating affinities for human serum albumin (log K_{HSA}) of the compounds **15–18** and their retention factors determined experimentally. These relationships are described by quadratic equations. In this case it is seen that only a significant increase in the logs k of the solutes of interest evokes a significant enhancement in their binding with albumin in the human serum. The strongest and statistically significant correlations were derived by plotting log K_{HSA} predictors versus the log k values determined on IAM column at 37 °C (R^2 = 0.9998 and 1.0000) and on ISRP column at 20 °C (R^2 = 0.9990 and 0.9998). Our results are consistent with some findings presented in earlier studies (Kaliszan et al., 1996; Ong et al., 1996; Caldwell et al., 1998; Nasal et al., 1994; Barbato et al., 2007; Stewart and Chan, 1998; Chan et al., 2005; Janicka and Pachuta-Stec, 2014) that described the advantages in bioactivity predictions of the retention parameters determined on IAM-type columns that imitate biosystems. In contrast, in the case of compounds **10–14** no effect of their lipophilicity on an optimal binding with human serum albumin was observed.

All the investigated small molecules (**10–18**) predicted to be highly permeable and therefore they are expected to be easily transported through the intestinal epithelium (according to the adopted classification of Caco-2 cell permeability (Yamashita et al., 2000; Yazdanian et al., 1998)). The computed Caco-2 values ranged from 218×10^{-6} cm s^{-1} for solute **14** to 241×10^{-6} cm s^{-1} for the most lipophilic compound **18**. In turn, the calculated $P_{e,\ jejunum}$ values ranged from 7.71×10^{-4} cm s^{-1} for analyte **13** to 7.96×10^{-4} cm s^{-1} for the parent compound **10**. These values indicate that all these solutes should be fast absorbed in the human jejunum at physiological pH (Stępnik et al., 2014). Nevertheless, in the case of all the compounds that were studied no influence of the logs k on Caco-2 as well as $P_{e,\ jejunum}$ predictors, respectively, was observed (Fig. S2 and Table S3 in Supplementary material).

Amongst this novel class of fused azaisocytosine-like congeners only molecules revealing the optimum lipophilicity range relevant to satisfactory pharmacokinetics may be regarded as the most promising candidates of the series for further *in vivo* testing. These lead structures emerged from a rational approach aiming at processing the experimental retention factors in bioactivity predictions. Statistically significant and highly predictive relationships presented in this study confirmed that the liquid chromatography with suitable reversed phase materials of diverse separation properties (including those imitating biosystems) is an excellent *in vitro* system that may be successfully used for assessing some fundamental pharmacokinetic properties (such as %F, $f_{u,\ plasma}$, log K_{HSA}) of our new solutes from their retention factors measured directly for given systems, as described above in detail. Pharmacokinetic properties of our novel compounds will be of value during their further *in vivo* investigations and finally all these descriptors of bioavailability could be validated in an animal model.

4. Conclusion

A novel class of fused azaisocytosine-containing congeners (**10–18**), as the anticipated false building blocks of nucleotides required for DNA synthesis, has been obtained employing the straightforward synthetic strategy. Their efficient and scalable synthesis was performed under mild reaction conditions with relatively good overall yields. All the original compounds demonstrated superior antiproliferative effects in three tumour cell lines to those of the commonly used folate antimetabolite – pemetrexed. The most promising candidates for designing more selective cytotoxic agents seem to be the representatives **12**, **13**, **14**, **15** and **18** as they reveal a lower toxicity for normal cells of the same epithelial origin after 24-h incubation period. The lipophilicity factors were determined by RPLC on three diverse stationary materials for all novel molecules and were used in correlation studies with *in silico* pharmacokinetic properties. A number of compounds also showed the optimum values of logs k significantly correlated with *in silico* bioactivity descriptors (such as %F – in the case of **10–18** and $f_{u,\ plasma}$, log K_{HSA} – in the case of **15–18**) required for the satisfactory pharmacokinetics *in vivo*. Therefore, these molecules seem to be the most promising lead structures that may be subjected to further more detailed drug development investigations.

Appendix A. Supplementary material

Supplementary data associated with this article can be found, in the online version, at http://dx.doi.org/10.1016/j.arabjc.2016.04.002.

References

Amidon, G.L., Lennernäs, H., Shah, V.P., Crison, J.R., 1995. A theoretical basis for a biopharmaceutic drug classification: the correlation of in vitro drug product dissolution and in vivo bioavailability. Pharm. Res. 12, 413–420.

Barbato, F., Cirocco, V., Grumetto, L., La Rotonda, M.I., 2007. Comparison between immobilized artificial membrane (IAM) HPLC data and lipophilicity in *n*-octanol for quinolone antibacterial agents. Eur. J. Pharm. Sci. 31, 288–297.

Bruliková, L., Džubák, P., Hajdúch, M., Hlaváč, J., 2011. Synthesis of various 5-alkoxymethyluracil analogues and structure–cytotoxic activity relationship study. Carbohydr. Res. 346, 2136–2144.

Caldwell, G.W., Masucci, J.A., Evangelisto, M., White, R., 1998. Evaluation of the immobilized artificial membrane phosphatidylcholine: Drug discovery column for high-performance liquid chromatographic screening of drug-membrane interactions. J. Chromatogr. A 800, 161–169.

Carrupt, P.A., Testa, B., Gaillard, P., 1997. Computational approaches to lipophilicity: methods and applications. Chapter 5. In: Lipkowitz, K.B., Boyd, D.B. (Eds.), . In: Reviews in Computational Chemistry, vol. 11. Wiley-VCH, J. Wiley and Sons Inc., New York.

Chan, E.C., Tan, W.L., Ho, P.C., Fang, L.J., 2005. Modeling Caco-2 permeability of drugs using immobilized artificial membrane chromatography and physicochemical descriptors. J. Chromatogr. A 1072, 159–168.

Cimpan, G., Hadaruga, M., Miclaus, V., 2000. Lipophilicity characterization by reversed-phase liquid chromatography of some furan derivatives. J. Chromatogr. A 869, 49–55.

Denny, W.A., 2001. Prodrug strategies in cancer therapy. Eur. J. Med. Chem. 36, 577–595.

Dill, K.A., Dorsey, J.G., 1994. The molecular mechanism of retention in reversed phase liquid chromatography. Chem. Rev. 66, 500–546.

Dorsey, J.G., Cooper, W.T., Wheeler, J.F., Barth, H.G., Foley, J.P., 1989. Liquid chromatography – theory and methodology. Anal. Chem. 89, 331–346.

Dorsey, J.G., Khaledi, M.G., 1993. Hydrophobicity estimations by reversed phase liquid chromatography – implications for biological partitioning processes. J. Chromatogr. A 656, 485–499.

Eartl, P., Rhode, B., Seltzer, P., 2000. Fast calculation of molecular polar surface area as a sum of fragment-based contributions and its application to the prediction of drug transport properties. J. Med. Chem. 43, 3714–3717.

Ellwart, J., Dormer, P., 1985. Effect of 5-fluoro-2′-deoxyuridine (FdUrd) on 5-bromo-2′-deoxyuridine (BrdUrd) incorporation into DNA measured with a monoclonal BrdUrd antibody and by the BrdUrd/Hoechst quenching effect. Cytometry 6, 513–520.

Fujita, T., Iwasa, J., Hansch, C., 1964. A new substituent constant π, derived from partition coefficients. J. Am. Chem. Soc. 86, 5157–5180.

Gocan, S., Cimpan, G., 2006. Lipophilicity measurements by liquid chromatography. J. Comer. Adv. Chromatogr. 44, 79–176.

Guerra, A., Campillo, N.E., Paez, J.A., 2010. Neural computational prediction of oral drug absorption based on CODES 2D descriptors. Eur. J. Med. Chem. 45, 930–940.

Hansch, C., Leo, A., 1979. A Substituent Constants for Correlation Analysis in Chemistry and Biology. Willey Interscience, New York.

Hawker Jr., J.R., 2003. Chemiluminescence-based BrdU ELISA to measure DNA synthesis. J. Immunol. Meth. 274, 77–82.

Hsieh, M.M., Dorsey, J.G., 1993. Accurate determination of log k_w in reversed-phased liquid chromatography. J. Chromatogr. 63, 163–178.

Huong, P.L., Kolk, A.H., Eggelte, T.A., Verstijnen, C.P., Gilis, H., Hendriks, J.T., 1991. Measurement of antigen specific lymphocyte proliferation using 5-bromo-deoxyuridine incorporation. An easy and low cost alternative to radioactive thymidine incorporation. J. Immunol. Meth. 140, 243–248.

Hwang, L.-C., Wang, C.-J., Lee, G.-H., Wang, Y., Tzeng, C.-C., 1995. Synthesis and structure assignment of 1-[(2-hydroxyethoxy) methyl]- and 1-[(1,3-dihydroxy-2-propoxy)methyl]-6-azaisocytosine. Heterocycles 41, 293–301.

Idaidek, N., Arafat, T., 2012. Saliva versus plasma pharmacokinetics: theory and application of a salivary excretion classification system. Mol. Pharm. 9, 2358–2363.

Janicka, M., Sztanke, M., Sztanke, K., 2013. Reversed-phase liquid chromatography with octadecylsilyl, immobilized artificial membrane and cholesterol columns in correlation studies with in silico biological descriptors of newly synthesized antiproliferative and analgesic active compounds. J. Chromatogr. A 1318, 92–101.

Janicka, M., Pachuta-Stec, A., 2014. Retention-property relationships of 1,2,4-triazoles by micellar and reversed-phase liquid chromatography. J. Sep. Sci. 37, 1419–1428.

Kaliszan, R., 2007. QSRR: Quantitative structure-(chromatographic) retention relationships. Chem. Rev. 107, 3212–3246.

Kaliszan, R., Nasal, A., Turowski, M., 1996. Quantitative structure-retention relationships in the examination of the topography of the binding site of antihistamine drugs on α_1-acid glycoprotein. J. Chromatogr. A 722, 25–32.

Kandefer-Szerszeń, M., Szuster-Ciesielska, A., Sztanke, K., Pasternak, K., 2014. 8-(4-Methoxyphenyl)-4-oxo-4,6,7,8-tetrahydroimidazo [2,1-c][1,2,4]triazin-3-formic acid hydrazide used as a drug for liver diseases. Polish Patent 216264.

Keisuke, M., Bonpei, Y., Masaak, M., Shintaro, I., Koichi, Y., 1993. Maillard reaction inhibitor, process for producing it, composition containing it and the use thereof. European Patent 0531812.

Klein, W., Kördel, W., Weiss, M., Poremski, H.J., 1988. Updating of the OECD Test Guideline 107 "partition coefficient n-octanol/water": OECD Laboratory intercomparison test on the HPLC method. Chemosphere 17, 361–386.

Lambert, W.J., 1993. Modeling oil-water partitioning and membrane permeation using reversed-phase chromatography. J. Chromatogr. A 656, 469–484.

Lipinski, C.A., Lombardo, F., Dominy, B.W., Feeney, P.J., 2001. Experimental and computational approaches to estimate solubility and permeability in drug discovery and development settings. Adv. Drug Deliv. Rev. 46, 3–26.

Magaud, J.P., Sargent, I., Mason, D.Y., 1988. Detection of human white cell proliferative responses by immunoenzymatic measurement of bromodeoxyuridine uptake. J. Immunol. Meth. 106, 95–100.

Matysiak, J., Karpińska, M.M., Skrzypek, A., Wietrzyk, J., Kłopotowska, D., Niewiadomy, A., Paw, B., Juszczak, M., Rzeski, W., 2015. Design, synthesis and antiproliferative activity against human cancer cell lines of novel benzo-, benzofuro-, azolo- and thieno-1,3-thiazinone resorcinol hybrids. Arab. J. Chem. http://dx.doi.org/10.1016/j.arabjc.2015.05.006.

Muir, D., Varon, S., Manthorpe, M., 1990. An enzyme-linked immunosorbent assay for bromodeoxyuridine incorporation using fixed microcultures. Anal. Biochem. 185, 377–382.

Nasal, A., Radwańska, A., Ośmiałowski, K., Buciński, A., Kaliszan, R., Barker, R., Sun, P., Hartwick, R.A., 1994. Quantitative relationships between the structure of beta-adrenolytic and antihistamine drugs and their retention on an alpha 1-acid glycoprotein HPLC column. Biomed. Chromatogr. 8, 125–129.

Ong, S., Lui, H., Pidgeon, C., 1996. Immobilized-artificial-membrane chromatography: measurements of membrane partition coefficient and predicting drug membrane permeability. J. Chromatogr. A 728, 113–128.

Palm, K., Stenberg, P., Luthman, K., Artursson, P., 1997. Polar molecular surface properties predict the intestinal absorption of drugs in humans. Pharm. Res. 14, 568–571.

Patrick, G.L., 2009. An Introduction to Medicinal Chemistry. Oxford University Press Inc., New York, USA.

Perisic-Janjic, N., Kaliszan, R., Wiczling, P., Milosevic, N., Uscumlic, G., Banjac, N., 2011. Reversed-phase TLC and HPLC retention data in correlation studies with in silico molecular descriptors and druglikeness properties of newly synthesized anticonvulsant succinimide derivatives. Mol. Pharm. 8, 555–563.

Pitha, J., Fiedler, P., Gut, J., 1966. Nucleic acids components and their analogues. LXXXIL. The fine structure of 6-azaisocytosine and its derivatives. Collect. Czech. Chem. Commun. 31, 1864–1871.

Rusinov, V.L., Ulomskii, E.N., Chupakhin, O.N., Charushkin, V.N., 2008. Azolo[5,1-c]1,2,4-triazines as a new class of antiviral compounds. Russ. Chem. Bull., Int. Ed. 57, 985–1014.

Stewart, B.H., Chan, O.H., 1998. Use of immobilized artificial membrane chromatography for drug transport applications. J. Pharm. Sci. 87, 1471–1478.

Stępnik, K.E., Malinowska, I., Rój, E., 2014. In vitro and in silico determination of oral, jejunum and Caco-2 human absorption of fatty acids and polyphenols. Micellar liquid chromatography. Talanta 130, 265–273.

Sztanke, K., 2012. New 1-substituted-2-hydrazino-4,5-dihydroimidazole hydroiodides and method for their obtaining. Polish Patent 211550.

Sztanke, K., Pasternak, K., Sztanke, M., Kandefer-Szerszeń, M., Kozioł, A.E., Dybała, I., 2009. Crystal structure, antitumour and antimetastatic activities of disubstituted fused 1,2,4-triazinones. Bioorg. Med. Chem. Lett. 19, 5095–5100.

Sztanke, M., Sztanke, K., 2014a. Mono and dichlorophenyl substituted 3-(4-nitrophenyl)-7,8-dihydroimidazo[2,1-c][1,2,4]triazin-4(6H)-ones, method for obtaining them and medical applications. Polish Patent, Appl. No 410363, 2014.

Sztanke, M., Sztanke, K., 2014b. Phenyl, alkylphenyl, dialkylphenyl, alkoxyphenyl substituted 3-(4-nitrophenyl)-7,8-dihydroimidazo[2,1-c][1,2,4]triazin-4(6H)-one derivatives, method for obtaining them and medical applications. Polish Patent, Appl. No 410364, 2014.

Sztanke, M., Rzymowska, J., Sztanke, K., 2015. Synthesis, structure elucidation and identification of antiproliferative activities of a novel class of thiophene bioisosteres bearing the privileged 7,8-dihydroimidazo[2,1-*c*][1,2,4]triazin-4(6*H*)-one scaffold. Bioorg. Med. Chem. 23, 3448–3456.

Szuster-Ciesielska, A., Sztanke, K., Kandefer-Szerszeń, M., 2012. A novel fused 1,2,4-triazine aryl derivative as antioxidant and nonselective antagonist of adenosine A_{2A} receptors in ethanol-activated liver stellate cells. Chem. Biol. Interact. 195, 18–24.

Taliani, S., Pugliesi, I., Barresi, E., Simorini, F., Salerno, S., La Motta, C., Marini, A.M., Cosimelli, B., Cosconati, S., Di Maro, S.,

Marinelli, Daniele, S., Trincavelli, M.L., Greco, G., Novellino, E., Martini, C., Da Settimo, F., 1998. 3-Aryl-[1,2,4]triazinobenzimidazol-4(10*H*)-one: a novel template for the design of highly selective A_{2B} adenosine receptor antagonists. J. Med. Chem. 55, 1490–1499.

Valko, K., 2004. Application of high-performance liquid chromatography based measurements of lipophilicity to model biological distribution. J. Chromatogr. A 1037, 299–310.

Van de Waterbeemd, H., Kansy, M., Wagner, B., Fischer, H., 1996. Lipophilicity measurement by reversed-phase high performance liquid chromatography (RP-HPLC). In: Pliska, V., Testa, B., van de Waterbeemd, H. (Eds.), . In: Lipophilicity in Drug Action and Toxicology. VCH Publishers Inc., New York, pp. 73–85.

Vega-Avila, B., Pugsley, M., 2011. An overview of colorimetric assay methods used to assess survival or proliferation of mammalian cells. Proc. West Pharmacol. Soc. 54, 10–14.

Vitha, M., Carr, P., 2006. The chemical interpretation and practice of linear solvation energy relationships in chromatography. J. Chromatogr. A 1126, 143–194.

Yamagami, C., Ogura, T., Nakao, N., 1990. Hydrophobicity parameters determined by reversed-phase liquid chromatography: I. Relationship between capacity factors and octanol-water partition coefficients for monosubstituted pyrazines and the related pyridines. J. Chromatogr. 514, 123–136.

Yamagami, C., Yokota, M., Takao, N., Alan, R., 1994. Hydrophobicity parameters determined by reversed-phase liquid chromatography. IX. Relationship between capacity factor and water-octanol partition coefficient of monosubstituted pyrimidines. Chem. Pharm. Bull. 42, 907–912.

Yamashita, S., Furubayashi, T., Kataoka, M., Sakane, T., Sezaki, H., Tokuda, H., 2000. Optimized conditions for prediction of intestinal drug permeability using Caco-2 cells. Eur. J. Pharm. 10, 195–204.

Yazdanian, M., Glynn, S.L., Wright, J.L., Hawi, A., 1998. Correlating partitioning and Caco-2 cell permeability of structurally diverse small molecular weight compounds. Pharm. Res. 15, 1490–1494.

Veber, D.E., Johnson, S.R., Cheng, H.-Y., Smith, B.R., Ward, K.W., Kopple, K.D., 2002. Molecular properties that influence the oral bioavailability of drug candidates. J. Med. Chem. 45, 2615–2623.

Please cite this article in press as: Sztanke, M. et al., Synthesis, structure elucidation, determination of antiproliferative activities, lipophilicity indices and pharmacokinetic properties of novel fused azaisocytosine-like congeners. Arabian Journal of Chemistry (2016), http://dx.doi.org/10.1016/j.arabjc.2016.04.002